Fine mapping without phenotyping: Identification of selection targets in secondary Evolve and Resequence experiments

Anna Maria Langmüller[1, 2], Marlies Dolezal[3], Christian Schlötterer[1, *]

[1] Institut für Populationsgenetik, Vetmeduni Vienna, Veterinärplatz 1, 1210 Vienna, Austria

[2] Vienna Graduate School of Population Genetics, Vetmeduni Vienna, Veterinärplatz 1, 1210 Vienna, Austria

[3] Plattform Bioinformatik und Biostatistik, Vetmeduni Vienna, Veterinärplatz 1, 1210 Vienna, Austria

*Author of Correspondence:

Christian Schlötterer, Institut für Populationsgenetik, Vetmeduni Vienna, Veterinärplatz 1, 1210 Vienna, Austria

+43 1 25077-4301, +43 1 25077-4390

christian.schloetterer@vetmeduni.ac.at

Abstract

Evolve and Resequence (E&R) studies investigate the genomic selection response of populations in an Experimental Evolution setup. Despite the popularity of E&R, empirical studies in sexually reproducing organisms typically suffer from an excess of candidate loci due to linkage disequilibrium, and single gene or SNP resolution is the exception rather than the rule. Recently, so-called "secondary E&R" has been suggested as promising experimental follow-up procedure to confirm putatively selected regions from a primary E&R study. Secondary E&R provides also the opportunity to increase mapping resolution by allowing for additional recombination events, which separate the selection target from neutral hitchhikers. Here, we use computer simulations to assess the effect of different crossing schemes, population size, experimental duration, and number of replicates on the power and resolution of secondary E&R. We find that the crossing scheme and population size are crucial factors determining power and resolution of secondary E&R: a simple crossing scheme with few founder lines consistently outcompetes crossing schemes where evolved populations from a primary E&R experiment are mixed with a complex ancestral founder population. Regardless of the experimental design tested, a population size of at least 4,800 individuals, which is roughly 5 times larger than population sizes in typical E&R studies, is required to achieve a power of at least 75%. Our study provides an important step towards improved experimental designs aiming to characterize causative SNPs in Experimental Evolution studies.

Keywords

Experimental Evolution, secondary Evolve and Resequence, experimental design, *Drosophila*, fine mapping

Significance

Despite the popularity of Evolve and Resequence (E&R) to investigate genomic selection responses, most studies that use sexually reproducing organisms have broad selection signatures and an excess of candidate loci due to linkage disequilibrium. In this study, we use computer simulations and statistical modelling to evaluate the effects of different experimental and population genetic parameters on the success of potential follow-up experiments (=secondary E&R) aiming to validate and fine-map selection signatures of primary studies. We found that a large population size in combination with a simple crossing scheme is key to the success of secondary E&R in *Drosophila*.

Introduction

Deciphering the genetic architecture of adaptation is one of the longstanding goals in evolutionary biology. Experimental Evolution (EE) has become a popular approach to study adaptation in real time (Garland & Rose 2009; Kawecki et al. 2012). In contrast to natural populations, EE offers the key advantage of replicating experiments under controlled laboratory conditions (Schlötterer et al. 2015). Evolve and Resequence (E&R) (Turner et al. 2011; Long et al. 2015; Schlötterer et al. 2015) – a combination of EE with Next Generation Sequencing – facilitates in-depth analysis of the genomic responses to selection, with the ultimate goal to identify and characterize individual adaptive loci.

E&R has already been successful in investigating genomic selection responses from standing genetic variation in adapting sexually reproducing organisms, such as chicken (Johansson et al. 2010), yeast (Burke et al. 2014), and *Drosophila* (Teotónio et al. 2009; Remolina et al. 2012; Martins et al. 2014; Barghi et al. 2019). Despite its popularity, E&R typically suffers from an excess of candidates caused by linkage disequilibrium between true

65 causative SNPs and neutral hitchhikers (Nuzhdin & Turner 2013; Tobler et al. 2014; Franssen
66 et al. 2015), which decreases the resolution of E&R studies and makes single gene resolution
67 (Martins et al. 2014) the exception rather than the rule.
68
69 The problem of candidate excess in E&R studies has been approached from different
70 angles. More refined statistical tests have been developed (Topa et al. 2015; Iranmehr et al.
71 2017; Kelly & Hughes 2019; Spitzer et al. 2020), and the combination of time-series data with
72 replicate populations has been identified as particularly powerful (Lang et al. 2013; Burke et
73 al. 2014; Barghi et al. 2020). Organisms with a higher recombination rate and a lack of large
74 segregating inversions that suppress recombination events have been suggested to be better
75 suited for E&R studies (Barghi et al. 2017). Computer simulations showed that the power of
76 E&R studies can be significantly improved by increasing the number of replicate populations,
77 the experimental duration, or by adjusting the applied selection regime (Baldwin-Brown et al.
78 2014; Kofler & Schlötterer 2014; Kessner & Novembre 2015; Vlachos & Kofler 2019).
79
80 Burny et al. (2020) recently suggested an experimental follow-up procedure
81 ("secondary E&R") to validate selection signals of primary E&R studies. The basic idea of
82 secondary E&R is that putative selection targets determined in the primary E&R study should
83 rise in frequency again when exposed to the same environmental conditions during an
84 additional E&R conducted after the primary experiment (Figure 1A). This experimental
85 validation of selection signals is especially attractive before starting the time-consuming
86 functional characterization of putatively selected alleles (e.g. based on the CRISPR/Cas
87 technology) (Gratz et al. 2013). A hitherto under-explored potential of secondary E&R is that
88 the additional recombination events during the secondary E&R can be used to fine map
89 selection signals of primary experiments. In addition to mixing evolved genotypes of a primary

90 E&R with non-adapted ancestral founder genotypes (coined "dilution" by Burny et al. (2020)),
91 we propose several different secondary E&R crossing schemes for validating and fine-mapping
92 of putative selection targets.
93
94 We evaluate the power and resolution of different secondary E&R designs to identify
95 causative SNPs via extensive computer simulations. We use logistic regression to assess which
96 simulated experimental and population genetic parameters have a significant effect on the
97 success of secondary E&R. Selection coefficient, dominance coefficient, and mean starting
98 allele frequency of the selection target all have a significant effect on the success of secondary
99 E&R. However, crossing scheme and population size emerge as the most influential parameters.
100 We show that the population size of secondary E&R experiments needs to be at least 5 times
101 larger than currently used population sizes in typical primary E&R studies with *Drosophila* to
102 achieve a power above 75%. Furthermore, we show that the crossing scheme is a crucial
103 experimental parameter shaping the power of secondary E&R - a simple crossing scheme with
104 few founder lines results in higher power and resolution compared to more complex crossing
105 schemes.
106
107 **Material & Methods**
108 Outline of the simulation framework
109 The non-adapted ancestral founder genotypes used in our simulation study are a randomly
110 chosen subset of 100 haplotypes from a panel of 189 sequenced *D. simulans* haplotypes
111 originally collected in Tallahassee (Florida, USA) capturing the amount of standing genetic
112 variation in a natural *Drosophila* population (Howie et al. 2019; Barghi et al. 2019). We use
113 the term "founder line" for an inbred isofemale line homozygous for one of these ancestral
114 haplotypes. In order to speed up the calculations, we only simulated chromosome-arm 2L.

115 Simulations with linkage were conducted with MimicrEE2 (v206) (Vlachos & Kofler 2018)
116 using the *D. simulans* recombination map (Howie et al. 2019). MimicrEE2 is a forward-
117 simulation framework for E&R studies that can simulate evolving experimental populations
118 based on their haplotype information and genome-wide recombination rates. We used the w-
119 mode of MimicrEE2 which computes the fitness of individuals directly from the selection
120 coefficients. If not stated otherwise, we simulated positive, additive selection for biallelic SNPs,
121 with selection coefficients being uniformly sampled between 0.07 and 0.1 for each positively
122 selected SNP and tracked the frequency of all SNPs over time (ranging from 479,507 to 970,466
123 SNPs, Table S1). We chose to simulate rather strong selection reasoning that alleles with a high
124 selection coefficient are more likely to be experimentally tested. On the other hand, strongly
125 selected alleles result in many neutral linked hitchhikers producing false positive signals that
126 adversely impact the mapping resolution (Kofler & Schlötterer 2014) - which requires follow-
127 up studies to identify the target of selection. If not stated otherwise, selected SNPs were
128 randomly chosen with an equal probability to be either co-dominant (dominance coefficient
129 h=0.5), or dominant (h=1). We did not consider recessive loci (h=0), because we do not
130 anticipate that fully recessive targets would result in sufficiently large allele frequency changes
131 to be detected in primary E&R experiments (Baldwin-Brown et al. 2014; Kofler & Schlötterer
132 2014). Similar to Baldwin-Brown et al. (2014), we did not model allele frequency estimation
133 errors caused for example by sequencing errors, limited read depth, read depth heterogeneity
134 across the chromosome, or the number of sequenced individuals. We used PoPoolation2 (Kofler
135 et al. 2011) to rescale allele counts for each biallelic position to a uniform read depth of 80.
136
137 Experimental parameters
138 The purpose of this study is to test the influence of different experimental parameters on the
139 power and resolution of secondary E&R. For this, we systematically varied the crossing

140 scheme, population size, experimental duration, and number of replicates to assess the effect of
141 these experimental parameters on the power and resolution of secondary E&R (Table 1).
142 We use the term "experimental design" to describe a distinct set of simulated experimental
143 parameters (e.g., crossing scheme=1:1_1f; population size=1,200 individuals; experimental
144 duration=60 generations; 5 replicates).
145
146 *Crossing scheme*
147 We simulated five different crossing schemes: 1:1 (versions 1f, 2f and 1f1nf), 1:few, 1:many,
148 dil:st, and dil:mt (Figure 1B-F). In the **1:1_1f** crossing scheme (Figure 1B), two inbred founder
149 lines are crossed at equal proportions. One inbred focal line carries a single target of selection
150 – known from a primary E&R experiment – and is crossed with inbred non-focal lines, not
151 carrying known adaptive alleles. We consider this a best-case scenario. Replicates are created
152 by crossing the same focal line to different non-focal lines without known targets of selection.
153 We used different non-focal lines as crossing partners to account for the possibility that in real
154 experiments these lines may contain unidentified selected loci. By using different lines, the
155 influence of selection targets present in a single non-focal line will be outweighed by the focal
156 locus, which is present in every replicate (Figure 1B). To further explore the influence of
157 unidentified selected loci, we simulated two more versions of the 1:1 crossing scheme with a
158 more realistic genetic architecture (Figure S1). In these versions, either the focal line itself, or
159 one of the non-focal lines carries one additional target of selection. We call these scenarios 2f,
160 for a total of 2 selected loci in the focal line (Figure S1B), and 1f1nf, for one selected locus in
161 the focal line and one selected locus in one of the non-focal lines (Figure S1C). For each
162 simulation, we sampled the selection coefficient of the additional selection target uniformly
163 between 0.07 and the selection coefficient of the selected SNP we consider for our analysis.
164 We simulated all possible combinations of dominance coefficients for the two selected SNPs

165 (0.5 – 0.5; 0.5 – 1; 1 – 0.5; 1 – 1). We ran 500 simulations for each of the 4 combinations of
166 dominance coefficients for 2f and 1f1nf, respectively.
167
168 In the **1:few** crossing scheme (Figure 1C) the focal line is crossed with a pool of five
169 non-focal lines that do not carry known beneficial alleles. The starting frequency of the focal
170 line is 50 %, whereas each non-focal line has a starting frequency of 10 %. Each replicate
171 consists of the same focal/non-focal line mixture. In the **1:many** crossing scheme (Figure 1D),
172 the focal line is crossed with a pool of 99 non-focal lines. Replicates consist of the same mixture
173 of lines, and the starting frequency of the focal line is 50 %.
174
175 It has been recently suggested, that "diluting" evolved populations of a primary E&R
176 experiment with many non-adapted ancestral genotypes of the very same primary E&R and
177 exposing the diluted populations to the same selection regime is a promising approach to
178 validate selection candidates (Burny et al. 2020). However, we lack a systematic power
179 assessment of such experiments with computer simulations. We thus included two "dilution"
180 crossing schemes (**dil:mt, dil:st**) into our analysis. To evaluate the power of dilution crossing
181 schemes, it is important to first simulate a primary E&R study. We chose to simulate a
182 population consisting of 100 different founder lines, a population size of 300 individuals, 60
183 generations of adaptation and one replicate, which can then be diluted with non-adapted
184 ancestral genotypes. SNPs in the primary E&R were tested for allele frequency change with the
185 χ^2 test.
186
187 The population of the **dil:st** crossing scheme carries only one beneficial SNP (**dil**:**st** =
188 **dil**ution: **s**ingle **t**arget, Figure 1E). The starting allele frequency of this beneficial, focal SNP is
189 sampled from the empirical starting allele frequency distribution of putatively selected alleles

190 from a previous E&R study in which *D. simulans* populations adapted to a new temperature
191 regime (mean starting frequency = 0.1) (Barghi et al. 2019). After simulating 60 generations of
192 adaptation (primary E&R), 50 % of the evolved population is replaced by flies of the non-
193 adapted ancestral founder population. After this dilution step, the secondary E&R was
194 simulated under the exact same selection regime as in the primary E&R. A region with a strong
195 selection signal from the primary E&R is chosen for validation in the dilution crossing schemes
196 (Burny et al. 2020). Hence, we investigated a 1 Mb window, which is the previously reported
197 median selected haplotype block length on chromosome-arm 2L (Barghi et al. 2019), around
198 the SNP with the highest χ^2 test-statistic in the primary E&R, in the secondary E&R.
199
200 The **dil:mt** (Figure 1F) crossing scheme has multiple selection targets (**dil**:**mt** =
201 **dil**ution: **m**ultiple **t**argets; 16 selection targets on chromosome-arm 2L (Barghi et al. 2019)).
202 Again, we investigate a 1 Mb window around the SNP with the highest χ^2 test statistic in the
203 primary E&R, in the secondary E&R. In case of multiple selection targets in the 1 Mb window,
204 we consider the target that is closest to the SNP with the highest CMH test statistic in the 1Mb
205 window of the secondary E&R in our analysis.

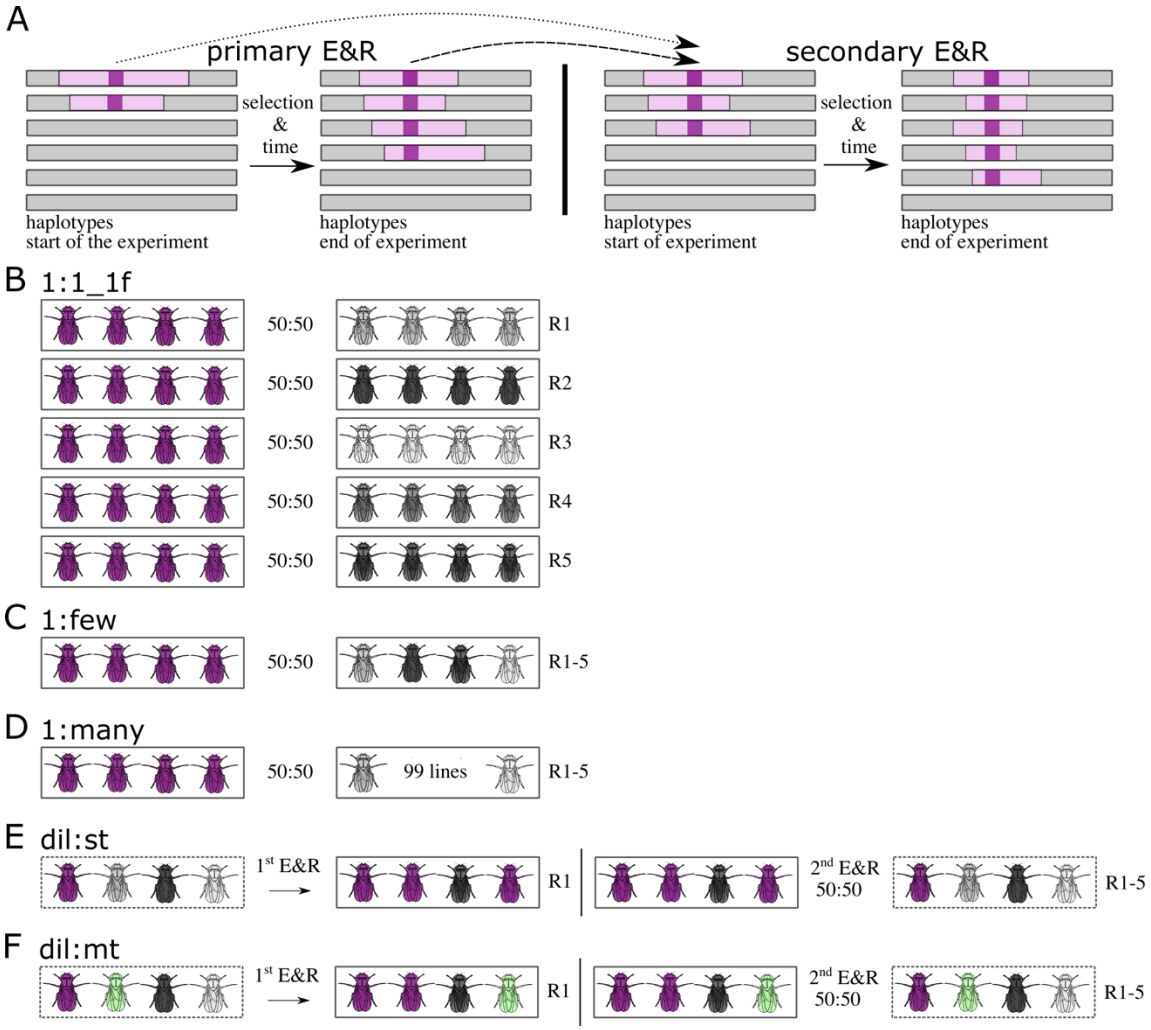

Figure 1. Basic idea of secondary Evolve and Resequence (E&R) and simulated crossing schemes. (A) The basic idea of secondary E&R is that a putative selection target (purple) determined in a primary E&R study (left) should rise in frequency again when exposed to the same environment (i.e., selection regime), during secondary E&R (right). Additional recombination events during the secondary E&R allow to fine map selected regions of primary E&R experiments (*i.e.,* reduce the number hitchhikers indicated in light pink) The two arrows indicate that the secondary E&R is either started with evolved haplotypes (dashed arrow) or with specific founder lines of the primary E&R (dotted arrow). (B) **1:1_1f** crossing scheme: Inbred flies with one target of selection (purple) are crossed to inbred flies without known beneficial variants. The starting frequency of each genotype is 50 %. In each replicate the line with the beneficial allele (focal line, purple) is crossed to a different line lacking beneficial mutations (non-focal lines, different shades of grey). (C) **1:few** crossing scheme: The focal line is crossed to a pool of flies with five different genotypes without known selection targets. The starting frequency of the focal line is again 50 %. (D) **1:many** crossing scheme: The focal line is crossed to a pool of 99 lines without known selection targets. (E) **dil:st** crossing scheme: 50 % of an evolved population originating from a primary E&R is replaced by ancestral genotypes of the primary E&R. The entire population has only one single target of selection (focal SNP, purple flies) (F) **dil:mt** crossing scheme: 50 % of an evolved population originating from a primary E&R is replaced by ancestral genotypes of the primary E&R. The ancestral population carries 16 targets of selection (flies carrying different beneficial SNPs are shown in purple, and green).

Population size

For two crossing schemes that are relatively easy to implement in empirical studies 1:1 (1f, 2f and 1f1nf) and dil:mt we performed simulations (experimental duration = 60 generations; 5 replicates) with independently sampled selection targets for population sizes of 300; 1,200; 4,800; and 19,200 individuals per replicate to test for the effect of the population size on the power and resolution of secondary E&R (Table 1). All other crossing schemes were evaluated at a population size of 300 individuals.

Experimental duration

All crossing schemes were evaluated after 60 generations. To explore the possibility that shorter experiments with less than 60 generations may already be sufficient to achieve satisfactory power, we analyzed the simulations for 1:1 (without 2f and 1f1nf) and dil:mt crossing schemes also already after 20 generations (Table 1).

Number of replicates

To assess the impact of the number of replicates on power of secondary E&R, we conducted for each crossing scheme (1:1 without 2f and 1f1nf) 100 additional simulations (population size= 300 individuals; experimental duration = 60 generations) with 30 replicates (Table 1).

244 **Table 1.** Simulation overview. 1:1_1f, 1:few, 1:many, dil:st, dil:mt: For each selected SNP, selection coefficients
245 were uniformly sampled between 0.07 and 0.1. Dominance coefficients were randomly chosen to be either 0.5
246 (co-dominant) or 1 (dominant). 1:1_2f, 1:1_1f1nf: For each simulation, the selection coefficient of the target of
247 interest was uniformly sampled between 0.07 and 0.1. In contrast to 1:1_1f, we simulated an additional selection
248 target, which was either located on the focal haplotype (1:1_2f) or one non-focal haplotype (1:1_1f1nf). The
249 selection coefficient of the additional selection target was uniformly sampled between 0.07 and the selection
250 coefficient of the target of interest. We simulated all possible combinations of dominance coefficients for the two
251 selected SNPs (500 simulations per combination).

Crossing scheme	Population size	Generations	Replicates	Number of simulations
1:1_1f	300; 1,200; 4,800; 19,200	60; 20	5/30	2,000/100
1:1_2f	300; 1,200; 4,800; 19,200	60	5	2,000
1:1_1f1nf	300; 1,200; 4,800; 19,200	60	5	2,000
1:few	300	60	5/30	2,000/100
1:many	300	60; 20	5/30	2,000/100
dil:st	300	60	5/30	2,000/100
dil:mt	300; 1,200; 4,800; 19,200	60; 20	5/30	2,000/100

252

253 Statistical analysis

254 All statistical analyses were performed using the R statistical computing environment (v3.5.3)
255 (R Core Team 3.5.3 2019).

256

257 *Power*

258 For each simulation, we tested all SNPs on chromosome-arm 2L for allele frequency increase
259 between the start and the end of the simulated secondary E&R using the Cochran-Mantel-
260 Haenszel-test (CMH-test, implemented in the R package poolSeq (v0.3.2) (Taus et al. 2017)).
261 The CMH-test allows to test for independence of matched data – e.g. allele counts of replicated
262 ancestral and evolved populations (Agresti & Kateri 2011). We ranked SNPs based on their
263 CMH test statistic using the dense ranking method in the R package data.table (v.1.12-8)

264 (Dowle & Srinivasan 2019). In dense ranking, SNPs with identical test statistics receive the
265 same rank, and the following SNP is assigned the immediately following rank.
266
267 Based on this ranking, we used two different approaches to classify simulations being
268 either successful, or unsuccessful. First, we only considered a simulation to be successful if the
269 true target of selection (i.e., the focal SNP with a selection coefficient > 0) was the SNP with
270 the highest test statistic (success-A). In a second analysis step, we classified a simulation as
271 success, if the focal target of selection was not more than 100 SNPs away from the SNP with
272 the highest test statistic (success-B, Figure 2). We acknowledge that success-B depends on the
273 maximum distance allowed between the true target of selection and the SNP with the highest
274 CMH test statistic (Figure 2). However, varying the maximum distance threshold did not alter
275 the relative performance of different experimental designs (data not shown). The power of an
276 experimental design is defined as the proportion of simulations that were able to detect the true
277 target of selection.

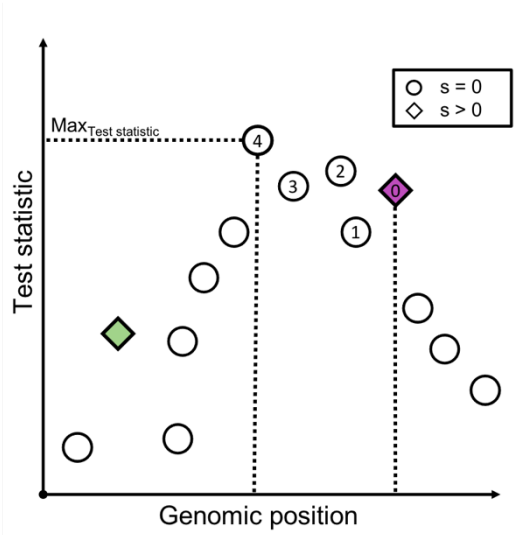

Figure 2. Schematic overview of the definition of success-B in a secondary Evolve and Resequence simulation. All SNPs (neutral = circle, beneficial = diamond) are tested for an allele frequency change with the Cochran-Mantel-Haenszel-test, and are ranked based on their test statistic (y-axis). If the focal selection target (purple diamond; one additional selected SNP is shown as green diamond - for crossing scheme 1:1_2f, 1:1_1fnf, and dil:mt) is less than 100 SNPs away from the SNP with the highest test statistic, the simulation run is deemed a success. In the example depicted, the distance in number of SNPs between the focal target of selection, and the SNP with the highest test statistic is 4, and the simulation is classified as success.

Resolution

For simulations where the selection target was detected (success-B), we determined the resolution of fine mapping of the selection target by counting the number of SNPs between the true selection target, and the SNP with the highest CMH test statistic.

Assessment of experimental and population genetic parameters

We used logistic regressions with a binomial error structure (ε) and a logit link function (Baayen 2008) to test how different experimental and population genetic parameters affect success and failure to identify targets of selection, i.e. success (Y) is treated as a binary response encoded in 0 (failure) and 1 (success) of secondary E&R.

We fitted three different models with R function *glm* with μ being the overall mean per model: Model 1 includes only the two crossing schemes 1:1_1f and dil:mt for which we also varied population size. Model 2 includes the three versions of crossing scheme 1:1 (1f, 2f and 1f1nf) at varying population sizes: 1f with only one positively selected SNP in the focal line; version 2f with two selected SNPs in the focal line; and version 1f1nf with one selected SNP in the focal line and one selected SNP in one non-focal line. Model 3 includes all 5 simulated crossing schemes (1:1 without 2f and 1f1nf) at a constant population size of 300 individuals.

Prior to model fitting, the two covariates selection coefficient and mean starting allele frequency (not applicable to model 2 as starting allele frequency is always 50%) were multiplied by 100, and z-transformed to a mean of zero and standard deviation of one for easier interpretable estimates (Schielzeth 2010).

(1) $Y_{ijklmn} = \mu + cross_i + h_j + s_k + af_l + N_m + (cross{:}h)_{ij} + (h{:}af)_{jl} + (cross{:}N)_{im} + (h{:}N)_{jm} + (cross{:}h{:}N)_{ijm} + \varepsilon_{ijklmn}$

(2) $Y_{ijkmn} = \mu + architecture_i + h_j + s_k + N_m + (architecture{:}h)_{ij} + (architecture{:}N)_{im} + (h{:}N)_{jm} + (architecture{:}h{:}N)_{ijm} + \varepsilon_{ijkmn}$

(3) $Y_{ijklm} = \mu + cross_i + h_j + s_k + af_l + (cross{:}h)_{ij} + (h{:}af)_{jl} + \varepsilon_{ijklm}$

Model 1 (equation (1)) contained (i) five explanatory variables as main effects; crossing scheme ($cross_i$), a fixed categorical effect with 2 levels - 1:1_1f and dil:mt; a fixed categorical effect of dominance coefficient (h_j) with levels 0.5 and 1; selection coefficient (s_k) and mean starting allele frequency (af_l) over replicated populations (both as continuous covariate); and

323 population size (N_m), a fixed categorical effect with 4 levels - 300; 1,200; 4,800; 19,200, (ii)
324 an interaction term between dominance coefficient and mean starting allele frequency
325 ($(h{:}\,af)_{jl}$), (iii) and a triple interaction between crossing scheme, dominance coefficient, and
326 population size ($(cross{:}\,h{:}\,N)_{ijm}$), and all pairwise interaction terms of effects involved in the
327 triple interaction term ($(cross{:}\,h)_{ij}$; $(cross{:}\,N)_{im}$; $(h{:}\,N)_{jm}$). We included interaction terms
328 into the model that have population genetic interpretations.
329
330 Data analyzed with model 1 contained 16,000 observations, namely 2,000 independent
331 simulation runs for each crossing scheme (1:1_1f, dil:mt), and each of the four different
332 population sizes (300; 1,200; 4,800; 19,200) (Table 1). To avoid potential bias introduced by
333 specific haplotypes being sampled, we randomly chose 4 sets of focal/non-focal founder lines
334 for the 1:1_1f crossing scheme and performed 500 simulation runs per set. The chosen set of
335 founder lines did not have a significant effect on the success of secondary E&R and is thus not
336 included in the final model (likelihood ratio test (LRT) full-reduced model comparison; data
337 not shown).
338
339 Model 2 (equation (2)) contained (i) four explanatory variables as main effects; a fixed
340 categorical effect "architecture" ($architecture_i$) that describes the version of the 1:1 crossing
341 scheme in combination with the dominance coefficient of the additional selected target (if
342 present) resulting in 5 levels: 1f; 2f_h05; 2f_h1; 1f1nf_h05; 1f1nf_h. Model 2 further contained
343 a fixed categorical effect of dominance coefficient for the focal SNP (h_j) with levels 0.5 and 1;
344 selection coefficient (s_k) as continuous covariate; and population size (N_m), a fixed categorical
345 effect with 4 levels: 300; 1,200; 4,800; 19,200, (ii) a triple interaction between architecture,
346 dominance coefficient, and population size ($(architecture{:}\,h{:}\,N)_{ijm}$), and all pairwise

interaction terms of effects involved in the triple interaction term $((architecture{:}\,h)_{ij}$; $(architecture{:}\,N)_{im}$; $(h{:}\,N)_{jm})$.

Data analyzed with model 2 contained 24,000 observations, namely 2,000 independent simulation runs for each version of the 1:1 crossing scheme (1f, 2f, 1f1nf), and four different population sizes (300; 1,200; 4,800; 19,200 individuals). Because model 1 showed that the chosen set of founder lines did not have a significant effect on the power of secondary E&R, we simulated only one set of focal/non-focal founder lines.

Model 3 (equation (3)) contained (i) four explanatory variables; crossing scheme ($cross_i$), a fixed categorical effect with 5 levels: 1:1_1f; 1:few; 1:many; dil:st; dil:mt, dominance coefficient (h_j), selection coefficient (s_k), and mean starting allele frequency (af_l) over replicated populations as main effects, as described for model 1, (ii) an interaction term between crossing scheme and dominance coefficient ($(cross{:}\,h)_{ij}$), (iii) and an interaction term between dominance coefficient and mean starting allele frequency ($(h{:}\,af)_{jl}$).

We analyzed 10,000 samples (2,000 independent simulation runs for each crossing scheme) (

366 Table *1*). For crossing schemes using only few different founder lines (1:1_1f, 1:few), the
367 simulation runs are based on 4 randomly chosen sets of founder lines each (500 simulation runs
368 per set). As in model 1, the set of founder lines does not have a significant effect on secondary
369 E&R success and is thus not included in the final model (LRT full-reduced model comparison;
370 data not shown). We performed additional analysis with 500 observations (100 independent
371 simulation runs for each crossing scheme) to determine the influence of the number of replicates
372 on the power of secondary E&R (Table 1).
373
374 We performed all diagnostic checks required for logistic regression. Absence of collinearity
375 was confirmed by computing the generalized Variance Inflation Factors (Fox & Monette 1992)
376 using function *vif* in R package *car* (v3.0-8 (Fox & Weisberg 2019)). Model stability was
377 checked with the R function *dfbeta*. For visualization, linear predictors (LP) were back-
378 transformed to success probabilities using the inverse logit transformation: $p_{sucess} = \frac{e^{LP}}{1+e^{LP}}$. 95
379 % confidence intervals of the fitted values were investigated with the R function *predict.glm*.
380 Significance of single explanatory variables was tested with a Type II ANOVA using function
381 *Anova* in R package car (Fox & Weisberg 2019) and are provided in the Supplement.
382 Significance of explanatory variables including all their modeled interactions was tested with a
383 likelihood ratio test comparing the full model with a nested reduced model with the same
384 structure as the full model, but lacking the assessed explanatory variable (and its interactions).
385 Significance is declared at an alpha cut-off of 5%. We used Nagelkerke's R^2 index (Nagelkerke
386 1991) to calculate the improvement of each model parameter upon the prediction of a reduced
387 model.
388
389 We observed two cases where a combination of explanatory variables resulted in complete
390 separation of data points (Figure 5A (dominance coefficient: 0.5, population size: 1,200,

391 architecture: 2f_h05), Figure S8A (dominance coefficient: 0.5, crossing scheme: dil:mt)). To
392 obtain interpretable model estimates, we added one pseudo-observation with the missing
393 response (success) to the data for each of these two cases.
394
395 **Data availability**
396 Information regarding the accessibility of raw sequence reads, phased haplotypes of the
397 ancestral *D. simulans* haplotypes as well as MimicrEE2 ready text files for the *D. simulans*
398 recombination map (file used in this project: Dsim_recombination_map_LOESS_100kb_1.txt)
399 can be found in (Howie et al. 2019). MimicrEE2 ready input files of the different experimental
400 designs, the simulated selection regimes, processed simulation results and all scripts that are
401 necessary to reproduce the results are available at SourceForge
402 (https://sourceforge.net/projects/secondary-e-r-sim/files/).
403
404 **Results**
405 We used forward simulations to assess the influence of different experimental and population
406 genetic parameters, more specifically crossing scheme, population size, dominance coefficient,
407 selection strength, and mean starting allele frequency on the success to detect and fine map
408 selection targets in secondary E&R experiments (Figure 1A). We used a Cochran-Mantel-
409 Haenszel (CMH) test to identify SNPs rising in allele frequency (number of SNPs see Table
410 S1). The CMH test allows to test for independence of matched categorical data (Agresti &
411 Kateri 2011), and compares favorably to other statistical methods in reliably identifying
412 possible targets of selection in E&R setups (Vlachos et al. 2019). A simulation run was
413 considered successful, if the true target of selection was the SNP with the highest CMH test
414 statistic (success-A). In a second analysis step, we considered simulation runs as successful, if
415 the true target of selection was not more than 100 SNPs away from the SNP with the highest

416 CMH test statistic (success-B, Figure 2). We used logistic regression to assess which
417 experimental and population genetic parameters have a significant effect on the success of
418 secondary E&R.
419
420 First, we evaluated two crossing schemes that can be easily implemented in empirical
421 studies, 1:1_1f (Figure 1B) and dil:mt (Figure 1F). The 1:1_1f crossing scheme (Figure 1B) is
422 based on founder lines only (a founder line is an inbred isofemale line homozygous for one
423 ancestral haplotype). Using information about the selected haplotype from a primary E&R
424 study, it is possible to determine which founder lines carry a selection target (Barghi et al.
425 2019). Note, this requires focal founder lines to be sequenced. Crossing a focal founder line
426 with the selected haplotype with a non-focal line without known selection targets offers the
427 advantage of reducing the number of selection targets dramatically. Using different non-focal
428 lines without known strong selection targets in each replicate reduces the potential of consistent
429 confounding effects of unidentified selection targets outside the region of interest – a signal the
430 CMH test is particularly sensitive to as it scans for consistent allele frequency changes across
431 replicates.
432
433 Dil:mt (Figure 1F) represents an entirely different approach. Dil:mt has multiple targets
434 of selection at different frequencies and is probably the simulated crossing scheme with the
435 most straight forward empirical implementation (Barghi et al. 2019; Burny et al. 2020). It is
436 based on a "dilution" approach, where evolved individuals from a primary E&R experiment are
437 crossed to the non-adapted ancestral founder population from the same primary E&R (Burny
438 et al. 2020). In contrast to 1:1_1f, a dil:mt crossing scheme requires both – ancestral and evolved
439 – populations of the primary E&R, but relatively limited information about selection targets on
440 individual founder lines.

441

442 To evaluate the 1:1_1f and dil:mt crossing scheme, we simulated secondary E&R
443 consisting of 5 replicated populations with constant population size (300; 1,200; 4,800, or
444 19,200 individuals per replicate) that evolve for 60 generations. We simulated positively
445 selected SNPs (selection coefficient is uniformly sampled between 0.07 and 0.1) that were
446 randomly chosen with equal probability to be either co-dominant (h=0.5) or dominant (h=1).
447 We used logistic regression to assess the effects of model parameters on secondary E&R
448 success (Model 1, *Assessment of experimental and population genetic parameters* in Material
449 & Methods). While selection strength (LRT full-reduced null model comparison (Model 1):
450 $\chi^2 = 67.4$, df = 1, p<0.001 (success-A); $\chi^2 = 73.4$, df = 1, p<0.001 (success-B)), dominance
451 coefficient (LRT full-reduced model comparison (Model 1): $\chi^2 = 733.4$, df = 9, p<0.001
452 (success-A); $\chi^2 = 714.5$, df = 9, p<0.001 (success-B)), and mean starting allele frequency
453 (LRT full-reduced model comparison (Model 1): $\chi^2 = 22.4$, df = 2, p<0.001 (success-A); $\chi^2 =$
454 17.4, df = 2, p<0.001 (success-B)) all have a significant effect on the power of secondary E&R
455 (Table S2), our analysis reveals that crossing scheme and population size have by far the
456 strongest influence on secondary E&R success. Both the crossing scheme (LRT full-reduced
457 model comparison (Model 1): $\chi^2 = 3510.1$, df = 8, p<0.001 (success-A); $\chi^2 = 3211.3$, df = 8,
458 p<0.001 (success-B)); and the population size (LRT full-reduced model comparison (Model 1):
459 $\chi^2 = 2142.9$, df = 12, p<0.001 (success-A); $\chi^2 = 2633.4$, df = 12, p<0.001 (success-B)) have
460 a significant effect on the success of secondary E&R, and are the only parameters with a
461 Nagelkerke's R^2 index above 0.2 (Table S3).

462

463 While a 1:1_1f crossing scheme results in higher power values than the dil:mt crossing
464 scheme independently of the population size, the difference to the dil:mt crossing scheme is
465 more pronounced in larger experimental populations (Figure 3). This does not hold only for the

power, but also for the resolution (= the distance in SNPs between the true target of selection, and the SNP with the highest CMH test statistic, Figure 4). A potential disadvantage of the 1:1_1f crossing scheme is that the low number of different founder lines (n=6, Figure 1B) causes more linkage disequilibrium, indicated by the number of neighboring SNPs with identical test statistics (=ties) and thus broadens signatures compared to dil:mt crossing scheme that has more founder lines (n=100) (Figure S2). However, this is outweighed by superior power of the 1:1_1f crossing scheme at every population size investigated (Figure 3-4).

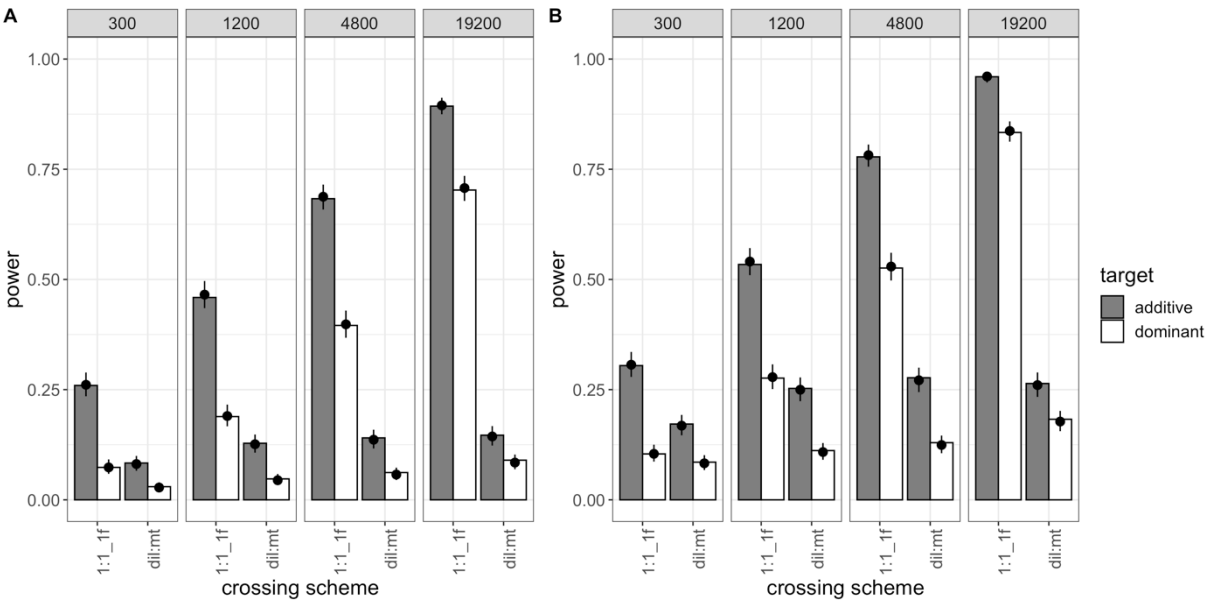

Figure 3. Power of the 1:1_1f and dil:mt crossing scheme at different population sizes (2,000 simulations/experimental design). Bars show the power (i.e., the proportion of successful simulations) separately for each combination of crossing scheme (1:1_1f, dil:mt), population size (300; 1,200; 4,800; 19,200 individuals), and dominance coefficient (additive in grey, dominant in white). The dots with error bars display the estimate from the fitted model (Model 1) and its 95 % confidence interval. For the model fit, the selection coefficient was fixed to its global average, and combination-specific average starting allele frequencies were used. (A) shows the results for success-A (= selection target is the SNP with the highest Cochran-Mantel-Haenszel (CMH) test statistic), (B) shows the results for success-B (= selection target is not more than 100 SNPs away from the SNP with the highest CMH test statistic).

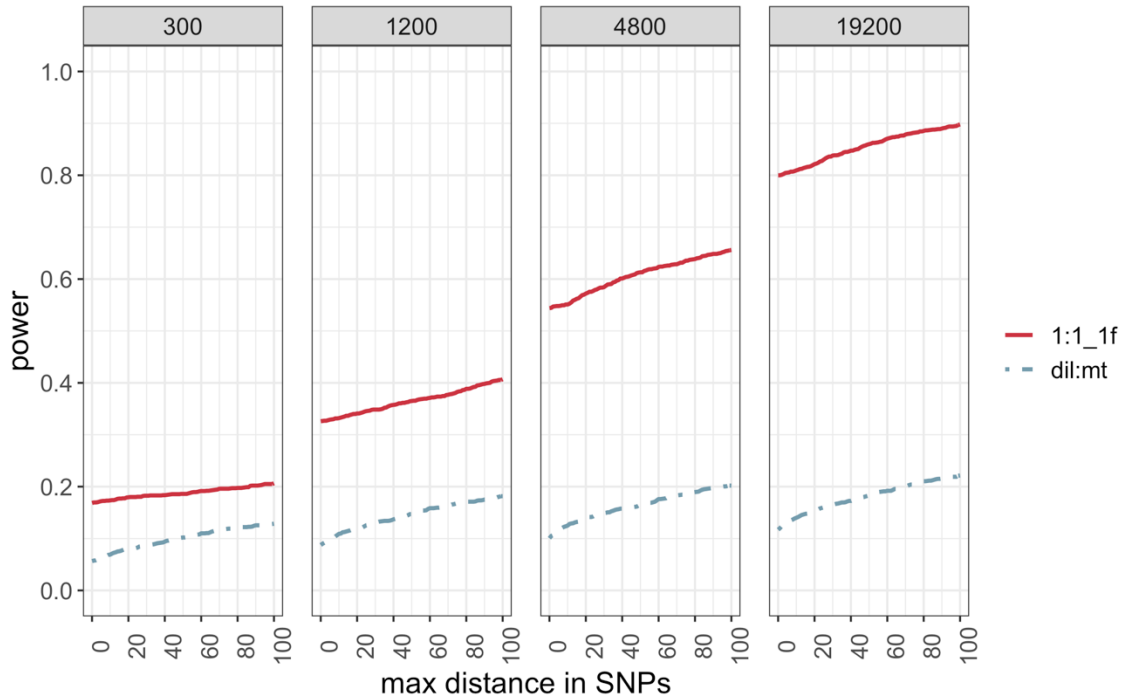

Figure 4. Resolution of the 1:1_f and dil:mt crossing scheme at different population sizes. Proportion of simulations (y-axis) that do not exceed a maximum distance in SNPs (x-axis) between the SNP with the highest Cochran-Mantel-Haenszel test statistic and the true target of selection. Each panel shows the result for one simulated population size.

Experimental duration

Our analysis showed that after 60 generations of adaptation, only experimental designs with a population size of at least 1,200 individuals have more power than 50 % (Figure 3). The 1:1_1f crossing scheme clearly outperforms dil:mt regardless of the population size, and reaches power above 75% only with a population size of at least 4,800 individuals. However, the maintenance of 5 replicates for 60 generations is labor intensive and can be quite time consuming for most sexual organisms. We explored the possibility that shorter experiments with less than 60 generations may already be sufficient to achieve satisfactory power values. We thus reanalyzed the power of the 1:1_1f, and dil:mt crossing scheme after 20 generations of adaptation (Table 1).

500 Consistent with previous computer simulation studies (Baldwin-Brown et al. 2014;
501 Kofler & Schlötterer 2014; Kessner & Novembre 2015) and empirical results (Langmüller &
502 Schlötterer 2020), we observe reduced power for experimental designs with shorter
503 experimental duration (Figure S3). Consistent with the results after 60 generations, the crossing
504 scheme (LRT full-reduced model comparison (Model 1): $\chi^2 = 2672.7$, df = 8, p<0.001
505 (success-A); $\chi^2 = 2234.4$, df = 8, p<0.001 (success-B)) and the population size (LRT full-
506 reduced model comparison (Model 1): $\chi^2 = 3176.4$, df = 12, p<0.001 (success-A); $\chi^2 =$
507 3375.3, df = 12, p<0.001 (success-B)) have the biggest effects on the success of secondary
508 E&R (TableS2-3).
509
510 In contrast to our analysis after 60 generations of adaptation, the dil:mt crossing scheme
511 results in higher power than the 1:1_1f crossing scheme for populations with the smallest
512 simulated population size (300 individuals) after 20 generations of adaptation (Figure S4). A
513 possible explanation for this is that the dil:mt crossing scheme has multiple beneficial targets.
514 Because we simulate additive selection, linked selection targets can act synergistically and
515 increase the frequency of the focal SNP over shorter time scales. This phenomenon of
516 pronounced allele frequency increase due to linked selection will be especially important if the
517 population size is small (i.e., drift is not neglectable), and the experimental duration is short.
518 This is reflected in a higher Nagelkerke's R^2 index for population size in secondary E&R with
519 an experimental duration of 20 generations compared to 60 generations of adaptation (Table
520 S3).
521
522 With increasing population size and thus, reduced genetic drift, the 1:1_1f crossing
523 scheme outcompetes dil:mt, as already seen in our analysis after 60 generations (Figure S3-4).
524 Although shorter experimental duration reduces power, our analysis after 20 generations of

525 adaptation highlights that if the maintenance of experimental populations for many generations
526 is not feasible, shorter experiments can achieve similar power if they are maintained at larger
527 population sizes (Figure 3, Figure S3).
528
529 Additional target of selection in the 1:1 crossing scheme
530 In contrast to dil:mt, the 1:1_1f crossing scheme harbors only one target of selection. We
531 simulated two additional versions of the 1:1 crossing scheme to investigate how one additional
532 target of selection influences the power of secondary E&R (Figure S1; Model 2, *Assessment of*
533 *experimental and population genetic parameters* in Material & Methods). We observed that
534 one additional beneficial SNP has a significant effect on the power of secondary E&R using
535 the 1:1 crossing scheme (LRT full-reduced model comparison (Model 2): $\chi^2 = 1727.7$, df =
536 32, p<0.001 (success-A); $\chi^2 = 2588.42$, df =32, p<0.001 (success-B); Table S4-5). This
537 significant effect is mainly driven by one scenario: when the focal line harbors two targets of
538 selection with the target of interest being dominant and the additional target being co-dominant
539 (Figure 5) the power to detect the target of interest is close to zero. The reason is that with a
540 starting frequency of 50 %, co-dominant alleles respond more to strong selection than dominant
541 alleles, because non-favored alleles are masked by high frequency dominant alleles (Figure S5).
542 This differential behavior is particularly pronounced for high allele frequencies. Note that our
543 definitions of success do not use prior information on the location of the focal SNP of interest.
544 We propose that a substantial fraction of the power can be recovered if the analysis is restricted
545 to the approximate location of the focal target determined in the primary E&R study. On the
546 other hand, for additive targets of interest one additional target of selection hardly reduces the
547 power of the 1:1 crossing scheme, regardless of the dominance coefficient of the additional
548 target and whether the additional target is positioned on the focal or one non-focal haplotype
549 (Figure 5). Overall, our results show that the 1:1 crossing scheme still outperforms dil:mt even

550 in the presence of one additional target of selection (Figure 3, Figure 5). For the remaining
551 analysis we will focus on a 1:1_1f crossing scheme with only one target of selection.
552

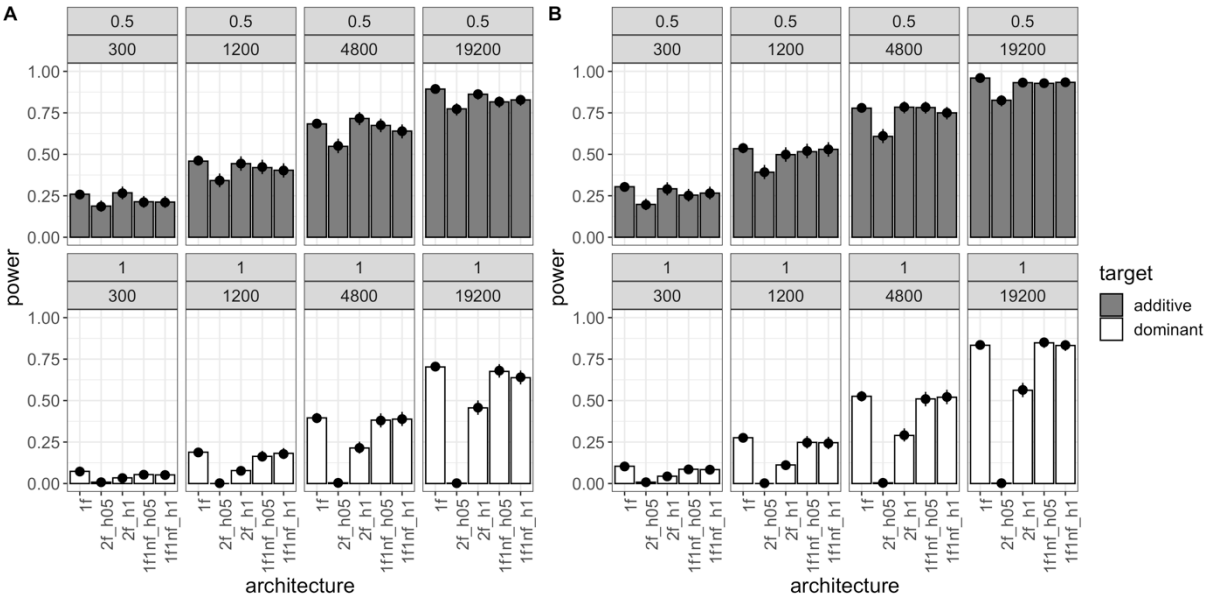

553 **Figure 5.** Power of the different 1:1 crossing schemes at different population sizes (Model 2) (2,000
554 simulations/experimental design) after 60 generations of adaptation. Bars show the power (i.e., proportion of
555 successful simulations) separately for each combination of 1:1 crossing scheme version with the dominance
556 coefficient of the additional target of selection: 1f, only one target of selection on the focal haplotype;
557 2f_h05/2f_h1, 2 targets of selection on the focal haplotype; 1f1nf_h05/1f1nf_h1, 1 target of selection on the focal
558 haplotype and one on one non-focal haplotype. Columns depict different population sizes (300; 1,200; 4,800;
559 19,200 individuals), and rows show different dominance coefficients of the target of interest (additive in top row,
560 dominant in bottom row). The dots with error bars display the model fit (Model 2) and its 95 % confidence interval.
561 For the model fit, the selection coefficient was fixed to its global average. (A) shows the results for success-A (=
562 selection target is the SNP with the highest Cochran-Mantel-Haenszel (CMH) test statistic) (B) shows the results
563 for success-B (= selection target is not more than 100 SNPs away from the SNP with the highest CMH test
564 statistic).
565

566 <u>Alternative crossing schemes</u>

567 Since large population sizes can be challenging to maintain, we also evaluated additional
568 crossing schemes which may perform better even for smaller population sizes (Model 3,
569 *Assessment of experimental and population genetic parameters* in Material & Methods). 1:few
570 (Figure 1C) is a modification of the 1:1_1f crossing scheme, which combines all non-focal lines
571 in each replicate - this provides a consistent genetic composition in each replicate. The 1:many

572 crossing scheme (Figure 1D) uses 1 focal, and 99 non-focal lines without selection target. We
573 reasoned that the larger number of segregating variants (970,466 SNPs compared to max
574 527,771 SNPs in 1:1 crossing scheme, Table S1) potentially provides a higher mapping
575 resolution. Finally, we modified the dilution crossing scheme by simulating only one selection
576 target in the founder population (dil:st, Figure 1E). Hence, no additional selection targets can
577 create potentially confounding selection signatures. For each experimental design, we
578 simulated a population size of 300 individuals, 60 generations of adaptation, and 5 replicates
579 (Table1).
580
581 Regardless of the experimental design, the simulated focal selection targets experienced
582 a pronounced allele frequency increase (Figure S6). In "dilution" crossing schemes (dil:st,
583 dil:mt; Figure 1E-F) the frequency trajectories of the focal SNPs were highly variable because
584 of the heterogeneous starting frequency. The crossing schemes where a single focal line with a
585 starting frequency of 50 % carries the beneficial allele typically had a superior performance
586 than dilution crossing schemes (Figure 6). Notably, the significant influence of crossing scheme
587 on secondary E&R success (LRT full-reduced model comparison (Model 3): $\chi^2 = 295.9$, df =
588 8, p<0.001 (success-A); $\chi^2 = 190.23$, df =8, p<0.001 (success-B)) (Table S6-7) cannot be
589 explained by a loss of the focal SNP in dilution crossing schemes, which occurred in less than
590 1 % of the simulations.
591
592 We found that the dil:st crossing scheme is still inferior to the 1:1_1f crossing scheme
593 for additive loci (Figure 6). Also, the modifications of the 1:1_1f crossing scheme (1:few,
594 1:many) do not provide a substantial improvement (Figure 6). Surprisingly, the 1:many crossing
595 scheme performed very poorly. This may be at least partly attributed to the larger number of
596 SNPs/kb, which will affect the SNP-based success rate (success-B, Figure 2). Given that the

three additional crossing schemes do not provide a clear advantage (Figure 6-7, Figure S7), and are not easier to execute experimentally, we did not evaluate them with larger population sizes.

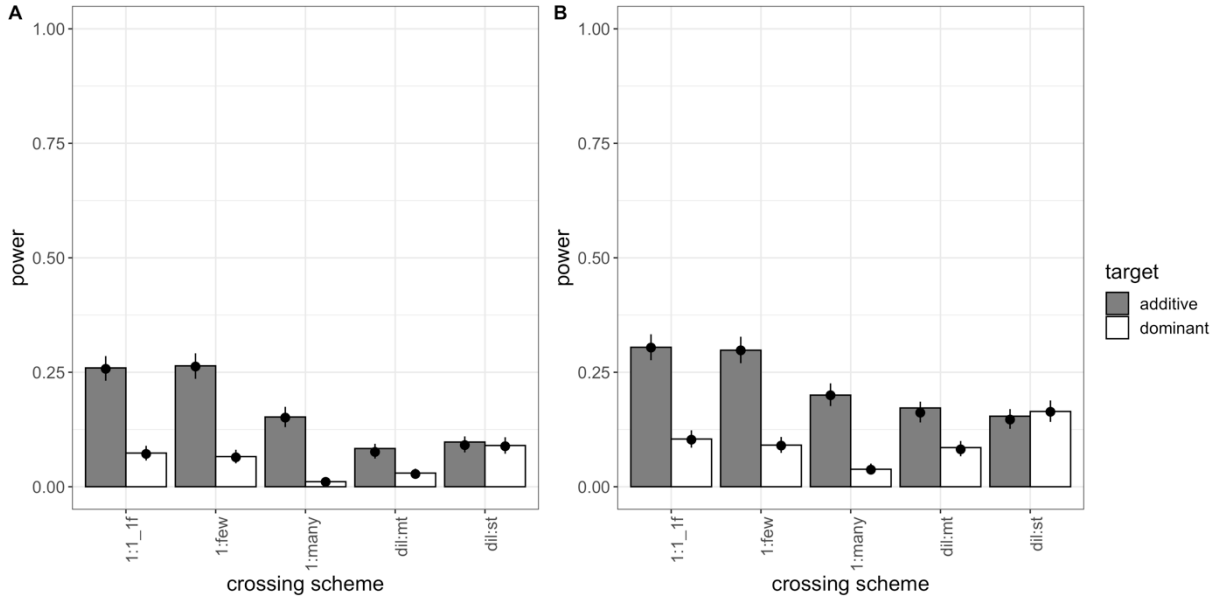

Figure 6. Power of five different crossing schemes (population size = 300 individuals; 2,000 simulations/experimental design). Bars show the power (i.e., proportion of successful simulations) separately for each combination of crossing scheme and dominance coefficient (additive in grey; dominant in white). The dots with error bars display the estimate from the fitted model (Model 3) and its 95 % confidence interval. For the model fit, the selection coefficient was fixed to its global average, and combination-specific average starting allele frequencies were used. (A) shows the results for success-A (= selection target is the SNP with the highest Cochran-Mantel-Haenszel (CMH) test statistic), (B) shows the results for success-B (= selection target is not more than 100 SNPs away from the SNP with the highest CMH test statistic).

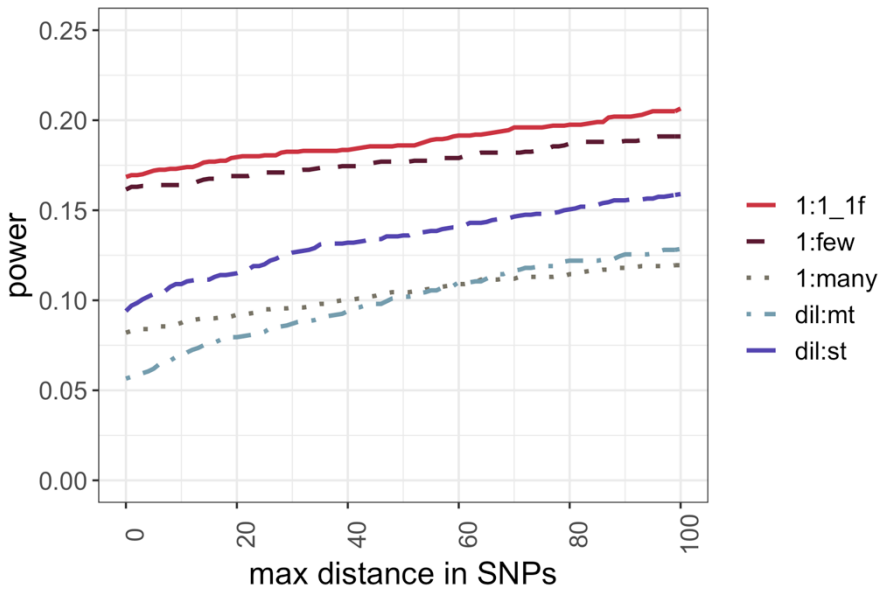

Figure 7. Resolution of five different crossing schemes. Proportion of simulations (y-axis) that do not exceed a maximum distance in SNPs (x-axis) between the SNP with the highest Cochran-Mantel-Haenszel test statistic and the true target of selection.

Number of replicates

Given the superior performance of experimental designs with larger population sizes (Figure 3), we were also interested whether more replicates with a smaller population size may provide further improvements. We performed additional simulations for all five different crossing schemes with a population size of 300 individuals per replicate, and 30 replicates (Table 1). Consistent with other simulation studies (Kofler & Schlötterer 2014; Kessner & Novembre 2015), more replicates result in increased power (Figure S8). The power of secondary E&R with 30 replicates (Table S6) is only significantly affected by the crossing scheme considering all modeled interactions (LRT full-reduced model comparison (Model 3): $\chi^2 = 31.467$, df = 8, p<0.001 (success-A); $\chi^2 = 16.692$, df = 8, p=0.033 (success-B); Table S7). The 1:1_1f crossing scheme with 30 replicates also has the highest resolution (Figure S9A). As expected, the impact of linkage disequilibrium, indicated by the number of ties, is dramatically reduced for all crossing schemes when more replicates are simulated (Figure S9B compared to Figure S7). However, similar improvements as seen with 30 replicates can be achieved if 5 replicates

627 of the 1:1_1f crossing scheme are used with a population size of 1,200 individuals (Figure 3).
628 Thus, the same power can be achieved while maintaining about 33 % fewer individuals.
629
630 Dominance coefficient, Selection coefficient, and mean starting allele frequency
631 As expected, dominance coefficient, selection coefficient, and average starting allele frequency
632 have a significant effect on the success of secondary E&R in all simulation scenarios, except
633 for data with 30 replicates. We observed that selection targets with a higher selection coefficient
634 and/or a higher mean starting allele frequency are easier to fine map. The lack of significant
635 effects of these parameters on secondary E&R success for the dataset with 30 replicates can
636 probably be explained by the smaller number of conducted simulations (100 for 30 replicates
637 and 2,000 for 5 replicates, Table 1). After crossing scheme and population size, the dominance
638 coefficient is the parameter with the highest Nagelkerke's R^2 index in our analysis, with
639 additive loci being easier to fine map. This is caused by the fact that heterozygotes and target
640 homozygotes with a dominant beneficial SNP have the same fitness, resulting in less efficient
641 selection that becomes especially apparent if the selected allele has already reached a high
642 frequency in the population, and non-selected allele homozygotes become rare (indicated by a
643 significant negative effect of the interaction term between dominance coefficient and mean
644 starting allele frequency in most of our statistical models).
645
646 **Discussion**
647 This work was inspired by the difficulty of most E&R studies with sexually reproducing
648 organisms to pinpoint selection targets, mostly due to numerous neutral hitchhikers resulting in
649 large haplotype blocks. Secondary E&R – a follow-up EE validating putative selection targets
650 of a primary E&R under an identical selection regime – has been recently suggested as
651 experimental approach for selection target confirmation (Burny et al. 2020). We used extensive

652 computer simulations to evaluate how experimental and population genetics parameter shape
653 the power and resolution of secondary E&R. As expected, dominance coefficient, selection
654 strength, and mean starting allele frequency of the selected target all have a significant effect
655 on the success of E&R, where dominant selection targets at high frequency are particularly
656 challenging to detect. However, population size and crossing scheme emerged as the most
657 influential parameters in our analysis.
658
659 The crossing scheme has a pronounced effect on secondary E&R success
660 We show that a simple crossing scheme, which only requires that (a subset of) the founder lines
661 are sequenced and that founder lines with and without the selection target of interest can be
662 distinguished, has the best power and resolution of the five crossing schemes tested. The 1:1
663 crossing scheme is particularly well-suited when many selection targets are detected in the
664 evolved populations of the primary E&R, because it uses only a subset of the lines from the
665 non-adapted ancestral founder population of the primary E&R study. This reduces potential
666 confounding effects between the selection target of interest and other adaptive loci in two ways.
667 First, non-adapted ancestral founder haplotypes will harbor on average less selection targets
668 than evolved haplotypes that can acquire multiple selection targets through recombination
669 events during the primary E&R (Otte & Schlötterer 2021). Because evolved haplotypes will
670 often harbor multiple selection targets, beneficial alleles will not propagate independently from
671 each other, which makes it challenging to fine-map single selection targets. Second, the total
672 number of potential beneficial alleles in a 1:1 crossing scheme is deliberately reduced by
673 picking only a subset of the founder lines of the primary E&R, which facilitates fine mapping
674 of one particular selection target of interest with secondary E&R.
675

676 We would like to point out that in our study "crossing schemes" are defined such that
677 they do not only differ in the actual crossing procedure, but also in the number and starting
678 allele frequency distribution of simulated selection targets (e.g., 1:1_1f vs. dil:mt). Additional
679 beneficial alleles can without doubt have an impact on the power of secondary E&R. While the
680 1:1 crossing scheme still outperforms dil:mt in the presence of one additional selection target,
681 the relative performance of crossing schemes might change given an even more complex
682 underlying genetic architecture. Furthermore, we focused in this study on the assessment of
683 experimental and population genetic parameters given a directional selection regime. Future
684 research on the potential of secondary E&R to fine map selection targets under a
685 complex/polygenic genetic architecture is needed, such as for example a quantitative trait under
686 stabilizing selection that experienced a recent shift in trait optimum.
687
688 Sufficient E&R power requires large population sizes
689 Our analyses also indicate that rather large population sizes are crucial to identify the causative
690 variant with sufficient confidence using a secondary E&R approach. This observation explains
691 why an empirical secondary E&R study in *D. simulans* with a population size of 1,250 flies per
692 replicated population failed to narrow down a pronounced candidate region from a primary
693 E&R in a secondary E&R after 30 generations, and only confirmed the presence of selected
694 alleles (Burny et al. 2020).
695
696 Our results suggest that large population sizes become especially crucial for short-term
697 secondary E&R. The low power of short-term E&R with reduced experimental duration (Kofler
698 & Schlötterer 2014) can be improved by a larger experimental population size. Our analyses
699 show that to achieve satisfactory power after only 20 generations requires population sizes of
700 tens of thousands of individuals– dimensions that are rather rare in current EE designs with

701 strictly sexually reproducing organisms, where population sizes are mostly limited by the
702 capacities to conduct such large experiments. Similar to previous simulation studies (Kofler &
703 Schlötterer 2014; Kessner & Novembre 2015), we demonstrated that increasing the number of
704 replicates results in more powerful secondary E&R. If large population sizes are not feasible,
705 maintaining many replicates at small population size can help to boost secondary E&R
706 performance. Additionally, the loss of one replicate in a highly replicated setup has a smaller
707 impact than in an experimental setup with very few replicates. However, we show that
708 additional replication cannot completely compensate the advantage of large population sizes in
709 secondary E&R. Based on this observation, we conclude that independent of the crossing
710 scheme, the power of secondary E&R will benefit from larger population sizes. Furthermore,
711 the resolution will significantly increase with more replicates – a result that we anticipate can
712 be generalized to different underlying genetic architectures as well as (model) organisms.
713
714 Allele frequency estimation errors and read depth
715 The results of this study are based on true allele frequencies estimated without error - a rather
716 optimistic assumption that will not hold for empirical data. In empirical E&R studies, numerous
717 factors influence the accuracy of allele frequency estimates, such as the rate of sequencing
718 errors, genome-wide read depth heterogeneity, and the average read depth (Baldwin-Brown et
719 al. 2014; Kofler & Schlötterer 2014; Tilk et al. 2019).
720
721 Individual whole-genome sequencing for entire populations becomes quickly
722 prohibitive with increasing sample size. Sequencing pools of individuals (Pool-Seq)
723 (Schlötterer et al. 2014) provides a cost-effective approach that allows to robustly estimate
724 allele frequency estimates and has become the method of choice for most E&R studies (Turner
725 et al. 2011; Schlötterer et al. 2015). Since typical Pool-Seq studies combine all individuals from

726 a given generation to reduce the sampling error (Schlötterer et al. 2014), the read depth of Pool-
727 Seq studies will affect all experimental designs to the same extent as long as the coverage is
728 considerably lower than the pool size.
729
730 Choice of model organism
731 Our simulations are parameterized for *D. simulans* because this species is better suited for E&R
732 studies than *D. melanogaster* (Barghi et al. 2017). While other species, such as *S. cerevisiae*
733 (Burke et al. 2014) or *C. remanei* (Castillo et al. 2015) have been used to study adaptive
734 response from standing genetic variation in outcrossing species, *Drosophila* is currently the
735 most popular organism. Nevertheless, we anticipate that the results of this study can be
736 generalized to other species, but the availability of sequenced inbred founder lines is probably
737 a more severe restriction, which could limit the widespread use of secondary E&R.
738
739 Selection regime
740 Our simulations are targeted for selection regimes with a moderate number of selection targets,
741 with rather strong effects, as seen in empirical E&R studies using *Drosophila* (e.g. Mallard et
742 al. 2018; Barghi et al. 2019; Michalak et al. 2019). Since strongly selected haplotype blocks
743 typically have low starting frequencies, we consider the 1:1 crossing scheme a very realistic
744 case, as most of the selection targets will be found only in a few ancestral founder lines. As
745 outlined above, evolved haplotypes in dil:mt on the other hand will most likely carry multiple
746 beneficial alleles that have recombined over the course of the primary E&R, which makes it
747 challenging to fine-map one distinct selection target of interest as our results suggest.
748
749 Furthermore, we assumed the rather simple selection scenario of directional selection.
750 More complex scenarios that include pleiotropy and/or epistasis were not considered. While

both are very important factors that could affect the allele frequency changes in an E&R study, we would like to point out that secondary E&R is designed to study loci, which experienced a substantial allele frequency increase in a primary experiment, thus pleiotropic constraints are not expected to be a major confounding factor. Epistasis, on the other hand may be more pronounced in the 1:1 crossing scheme. It may be possible that the focal allele is only selected in a subset of the replicates, but not in others-or the response may differ between replicates. While this reduces the power of secondary E&R to fine-map the selection target, such a result may open the possibility to study the impact of epistatic effects. Since the founder lines will be available, it will be possible to repeat the experiment with replication for each genotype combination to assure that the heterogeneous response comes from epistatic effects and is not linked to stochastic changes.

Finally, it is important to keep in mind that the secondary E&R designs discussed here are not tailored to study highly polygenic traits, because in this study we were assuming that recombination facilitates the identification of a selection target with a major effect. For a highly polygenic trait, selected haplotype blocks identified in the primary E&R experiment (with multiple selected loci) would be broken down during the secondary E&R, which reduces their selective advantage. To what extent this different behavior in secondary E&R experiments can be used to distinguish these different architectures requires further work.

Acknowledgements

We thank the members of the Institute of Population Genetics for fruitful discussion and support. Thanks to Roger Mundry who shared R scripts for the statistical analyses. Special thanks to Rupert Mazzucco, Robert Kofler, Kathrin Otte, and Christos Vlachos for their support regarding the computer simulations. Special thanks to Claire Burny and Robert Kofler for

helpful comments on earlier versions of the manuscript. Last, but not least we are thankful to the anonymous reviewers for their constructive feedback. This work was supported by the Austrian Science Funds (FWF) [grant numbers W1225, P-32935]; and by the European Research Council (ERC) [grant ArchAdapt].

Authors Contribution

AML, MD, and CS designed the analysis. AML performed the forward simulations, and the bioinformatic analysis. AML, and MD performed the statistical analysis. AML, MD, and CS wrote the manuscript.

785 **References**

786 Agresti A, Kateri M. 2011. Categorical Data Analysis. In: International Encyclopedia of
787 Statistical Science. Lovric, M, editor. Springer Berlin Heidelberg: Berlin, Heidelberg pp.
788 206–208. doi: 10.1007/978-3-642-04898-2_161.

789 Baayen RH. 2008. *Analyzing Linguistic Data: A Practical Introduction to Statistics using R*.
790 Cambridge University Press doi: 10.1017/CBO9780511801686.

791 Baldwin-Brown JG, Long AD, Thornton KR. 2014. The Power to Detect Quantitative Trait
792 Loci Using Resequenced, Experimentally Evolved Populations of Diploid, Sexual Organisms.
793 Mol. Biol. Evol. 31:1040–1055. doi: 10.1093/molbev/msu048.

794 Barghi N et al. 2019. Genetic redundancy fuels polygenic adaptation in *Drosophila*. PLOS
795 Biol. 17:1–31. doi: 10.1371/journal.pbio.3000128.

796 Barghi N, Hermisson J, Schlötterer C. 2020. Polygenic adaptation: a unifying framework to
797 understand positive selection. Nat. Rev. Genet. 21:769–781. doi:
798 https://doi.org/10.1038/s41576-020-0250-z.

799 Barghi N, Tobler R, Nolte V, Schlötterer C. 2017. *Drosophila simulans* : A Species with
800 Improved Resolution in Evolve and Resequence Studies. G3 Genes|Genomes|Genetics.
801 7:2337–2343. doi: 10.1534/g3.117.043349.

802 Burke MK, Liti G, Long AD. 2014. Standing Genetic Variation Drives Repeatable
803 Experimental Evolution in Outcrossing Populations of *Saccharomyces cerevisiae*. Mol. Biol.
804 Evol. 31:3228–3239. doi: 10.1093/molbev/msu256.

805 Burny C et al. 2020. Secondary Evolve and Resequencing: An Experimental Confirmation of
806 Putative Selection Targets without Phenotyping. Genome Biol. Evol. 12:151–159. doi:
807 10.1093/gbe/evaa036.

808 Castillo DM, Burger MK, Lively CM, Delph LF. 2015. Experimental evolution: Assortative
809 mating and sexual selection, independent of local adaptation, lead to reproductive isolation in

810 the nematode Caenorhabditis remanei. Evolution. 69:3141–3155. doi: 10.1111/evo.12815.
811 Dowle M, Srinivasan A. 2019. data.table: Extension of `data.frame`. https://cran.r-
812 project.org/package=data.table.
813 Fox J, Monette G. 1992. Generalized Collinearity Diagnostics. J. Am. Stat. Assoc. 87:178–
814 183. http://www.jstor.org/stable/2290467.
815 Fox J, Weisberg S. 2019. *An R Companion to Applied Regression*. Third. Sage
816 https://socialsciences.mcmaster.ca/jfox/Books/Companion/.
817 Franssen SU, Nolte V, Tobler R, Schlötterer C. 2015. Patterns of Linkage Disequilibrium and
818 Long Range Hitchhiking in Evolving Experimental *Drosophila melanogaster* Populations.
819 Mol. Biol. Evol. 32:495–509. doi: 10.1093/molbev/msu320.
820 Garland T, Rose M. 2009. *Experimental Evolution: Concepts, Methods, and Applications of*
821 *Selection Experiments*.
822 Gratz SJ et al. 2013. Genome engineering of *Drosophila* with the CRISPR RNA-guided Cas9
823 nuclease. Genetics. 194:1029–1035. doi: 10.1534/genetics.113.152710.
824 Howie JM, Mazzucco R, Taus T, Nolte V, Schlötterer C. 2019. DNA Motifs Are Not General
825 Predictors of Recombination in Two *Drosophila* Sister Species. Genome Biol. Evol.
826 11:1345–1357. doi: 10.1093/gbe/evz082.
827 Iranmehr A, Akbari A, Schlötterer C, Bafna V. 2017. CLEAR: Composition of Likelihoods
828 for Evolve and Resequence Experiments. Genetics. 206:1011–1023. doi:
829 10.1534/genetics.116.197566.
830 Johansson AM, Pettersson ME, Siegel PB, Carlborg Ö. 2010. Genome-Wide Effects of Long-
831 Term Divergent Selection. PLOS Genet. 6:e1001188. doi: 10.1371/journal.pgen.1001188.
832 Kawecki TJ et al. 2012. Experimental evolution. Trends Ecol. Evol. 27:547–560. doi:
833 10.1016/j.tree.2012.06.001.
834 Kelly JK, Hughes KA. 2019. Pervasive Linked Selection and Intermediate-Frequency Alleles

835 Are Implicated in an Evolve-and-Resequencing Experiment of *Drosophila simulans*.
836 Genetics. 211:943–961. doi: 10.1534/genetics.118.301824.
837 Kessner D, Novembre J. 2015. Power analysis of artificial selection experiments using
838 efficient whole genome simulation of quantitative traits. Genetics. 199:991–1005. doi:
839 10.1534/genetics.115.175075.
840 Kofler R, Pandey RV, Schlötterer C. 2011. PoPoolation2: identifying differentiation between
841 populations using sequencing of pooled DNA samples (Pool-Seq). Bioinformatics. 27:3435–
842 3436. doi: 10.1093/bioinformatics/btr589.
843 Kofler R, Schlötterer C. 2014. A guide for the design of evolve and resequencing studies.
844 Mol. Biol. Evol. 31:474–483. doi: 10.1093/molbev/mst221.
845 Lang GI et al. 2013. Pervasive genetic hitchhiking and clonal interference in forty evolving
846 yeast populations. Nature. 500:571–574. doi: 10.1038/nature12344.
847 Langmüller AM, Schlötterer C. 2020. Low concordance of short-term and long-term selection
848 responses in experimental Drosophila populations. Mol. Ecol. 29:3466–3475. doi:
849 10.1111/mec.15579.
850 Long A, Liti G, Luptak A, Tenaillon O. 2015. Elucidating the molecular architecture of
851 adaptation via evolve and resequence experiments. Nat. Publ. Gr. 16:567–582. doi:
852 10.1038/nrg3937.
853 Mallard F, Nolte V, Tobler R, Kapun M, Schlötterer C. 2018. A simple genetic basis of
854 adaptation to a novel thermal environment results in complex metabolic rewiring in
855 *Drosophila*. Genome Biol. 19:119. doi: 10.1186/s13059-018-1503-4.
856 Martins NE et al. 2014. Host adaptation to viruses relies on few genes with different cross-
857 resistance properties. Proc. Natl. Acad. Sci. U. S. A. 111:5938–43. doi:
858 10.1073/pnas.1400378111.
859 Michalak P, Kang L, Schou MF, Garner HR, Loeschcke V. 2019. Genomic signatures of

experimental adaptive radiation in *Drosophila*. Mol. Ecol. 28:600–614. doi: https://doi.org/10.1111/mec.14917.

Nagelkerke N. 1991. A note on a general definition of the coefficient of determination. Biometrika. 78:691–692.

Nuzhdin S V, Turner TL. 2013. Promises and limitations of hitchhiking mapping. Curr. Opin. Genet. Dev. 23:694–699. doi: 10.1016/j.gde.2013.10.002.

Otte KA, Schlötterer C. 2021. Detecting selected haplotype blocks in evolve and resequence experiments. Mol. Ecol. Resour. 21:93–109. doi: 10.1111/1755-0998.13244.

R Core Team 3.5.3. 2019. A Language and Environment for Statistical Computing. R Found. Stat. Comput. 2:https://www.R-project.org. http://www.r-project.org.

Remolina SC, Chang PL, Leips J, Nuzhdin S V, Hughes KA. 2012. Genomic basis of aging and life-history evolution in *Drosophila melanogaster*. Evolution. 66:3390–3403. doi: 10.1111/j.1558-5646.2012.01710.x.

Schielzeth H. 2010. Simple means to improve the interpretability of regression coefficients. Methods Ecol. Evol. 1:103–113. doi: 10.1111/j.2041-210X.2010.00012.x.

Schlötterer C, Kofler R, Versace E, Tobler R, Franssen SU. 2015. Combining experimental evolution with next-generation sequencing: a powerful tool to study adaptation from standing genetic variation. Heredity (Edinb). 114:431–440. doi: 10.1038/hdy.2014.86.

Schlötterer C, Tobler R, Kofler R, Nolte V. 2014. Sequencing pools of individuals — mining genome-wide polymorphism data without big funding. Nat. Rev. Genet. 15:749–763. doi: 10.1038/nrg3803.

Spitzer K, Pelizzola M, Futschik A. 2020. Modifying the Chi-square and the CMH test for population genetic inference: Adapting to overdispersion. Ann. Appl. Stat. 14:202–220. doi: 10.1214/19-AOAS1301.

Taus T, Futschik A, Schlötterer C. 2017. Quantifying selection with pool-seq time series data.

885 Mol. Biol. Evol. 34:3023–3034. doi: 10.1093/molbev/msx225MBE.
886 Teotónio H, Chelo IM, Bradić M, Rose MR, Long AD. 2009. Experimental evolution reveals
887 natural selection on standing genetic variation. Nat. Genet. 41:251–257. doi: 10.1038/ng.289.
888 Tilk S et al. 2019. Accurate Allele Frequencies from Ultra-low Coverage Pool-Seq Samples
889 in Evolve-and-Resequence Experiments. G3 Genes|Genomes|Genetics. 9:4159–4168. doi:
890 10.1534/g3.119.400755.
891 Tobler R et al. 2014. Massive Habitat-Specific Genomic Response in *D. melanogaster*
892 Populations during Experimental Evolution in Hot and Cold Environments. Mol. Biol. Evol.
893 31:364–375. doi: 10.1093/molbev/mst205.
894 Topa H, Jónás Á, Kofler R, Kosiol C, Honkela A. 2015. Gaussian process test for high-
895 throughput sequencing time series: Application to experimental evolution. Bioinformatics.
896 31:1762–1770. doi: 10.1093/bioinformatics/btv014.
897 Turner TL, Stewart AD, Fields AT, Rice WR, Tarone AM. 2011. Population-Based
898 Resequencing of Experimentally Evolved Populations Reveals the Genetic Basis of Body
899 Size Variation in *Drosophila melanogaster*. PLoS Genet. 7:e1001336. doi:
900 10.1371/journal.pgen.1001336.
901 Vlachos C et al. 2019. Benchmarking software tools for detecting and quantifying selection in
902 evolve and resequencing studies. Genome Biol. 20:169. doi: 10.1186/s13059-019-1770-8.
903 Vlachos C, Kofler R. 2018. MimicrEE2: Genome-wide forward simulations of Evolve and
904 Resequencing studies. PLOS Comput. Biol. 14:e1006413.
905 https://doi.org/10.1371/journal.pcbi.1006413.
906 Vlachos C, Kofler R. 2019. Optimizing the Power to Identify the Genetic Basis of Complex
907 Traits with Evolve and Resequence Studies. Mol. Biol. Evol. 36:2890–2905. doi:
908 10.1093/molbev/msz183.
909

Supplementary Figures

Figure S1. Simulated versions of the 1:1 crossing scheme.

Figure S2. Number of ties in the 1:1_1f and dil:mt crossing schemes.

Figure S3. Power of the 1:1_1f and dil:mt crossing schemes after 20 generations of adaptation.

Figure S4. Resolution of the 1:1_1f and dil:mt crossing schemes after 20 generations of adaptation.

Figure S5. Allele frequency trajectories of selected SNPs in 1:1_2f.

Figure S6. Allele frequency trajectories of focal SNPs in 5 different crossing schemes.

Figure S7. Number of ties in 5 different crossing schemes.

Figure S8. Power of 5 different crossing schemes with 30 replicates per simulation.

Figure S9. Resolution of 5 different crossing schemes with 30 replicates per simulation.

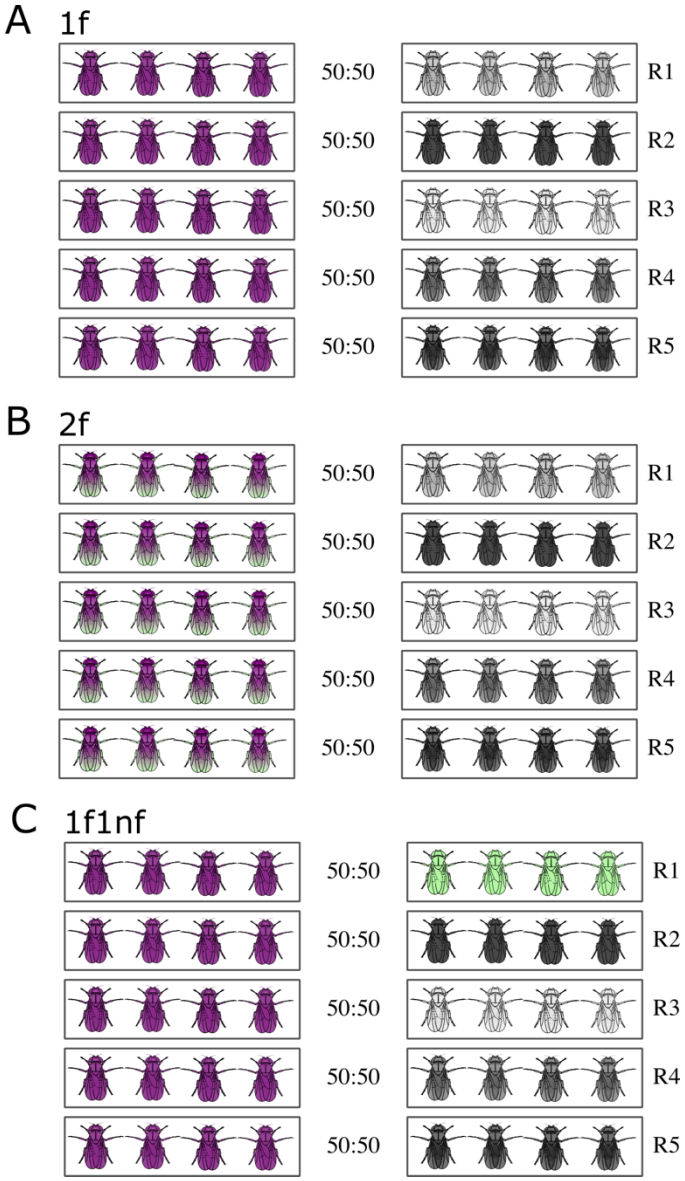

Figure S1. Simulated versions of the 1:1 crossing scheme. (A) Default version of the 1:1 crossing scheme (=**1f** for 1 focal SNP). Inbred flies with one target of selection (purple) are crossed to inbred flies without known beneficial variants. The starting frequency of each genotype is 50%. In each replicate the line with the beneficial allele (focal line, purple) is crossed to a different line lacking beneficial mutations (non-focal lines are colored in different shades of grey). Figure S1A is equal to Figure 1B in the main manuscript. (B) 2 focal SNPs (=**2f**) version of the 1:1 crossing scheme. The focal line carries two beneficial variants: the focal SNP we aim to fine map (purple) and one additional target of selection (green). (C) 1 focal, 1 non-focal SNP (=**1f1nf**) version of the 1:1 crossing scheme: One non-focal line carries on additional beneficial variant (green).

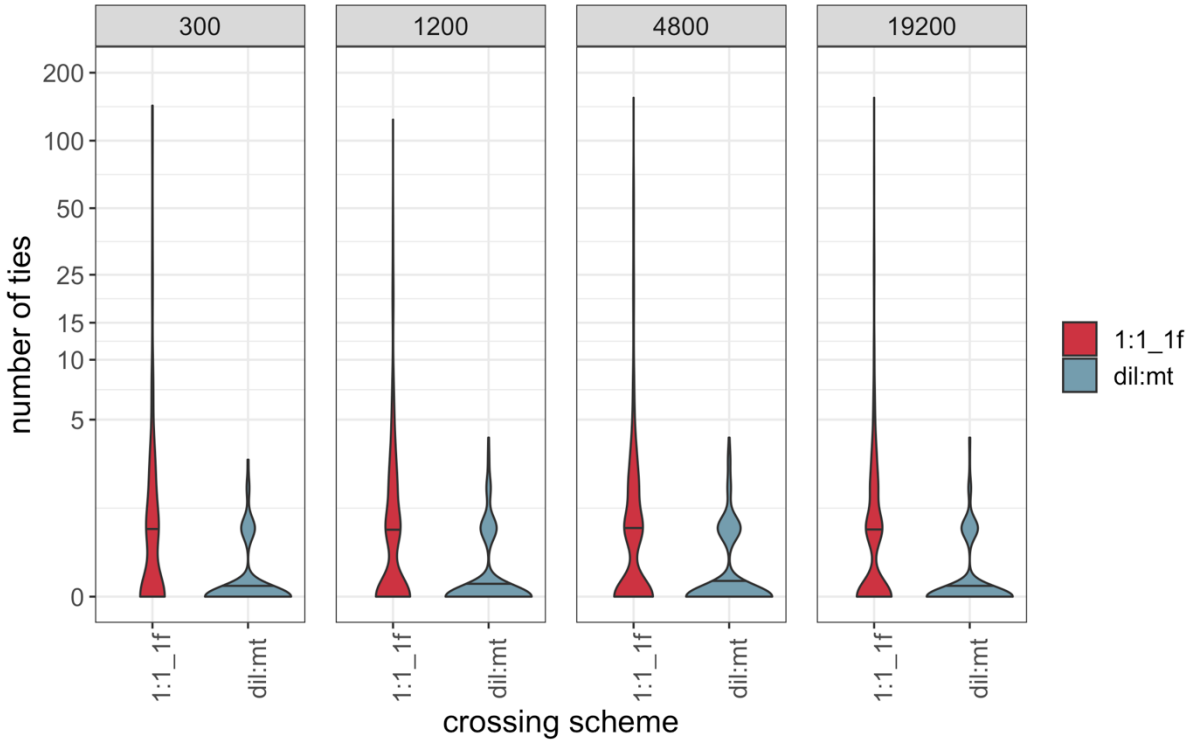

Figure S2. Violin plots of the number of ties (y axis = $\log_{10}$ (number of ties + 1)) for simulations where the true target of selection has the highest Cochran-Mantel-Haenszel (CMH) test statistic (success-A). The black horizontal lines in the violin plots display the median number of observed ties. Each panel shows the results for one particular simulated population size. Ties are defined as neighboring SNPs that have the same CMH test statistic as the target of selection.

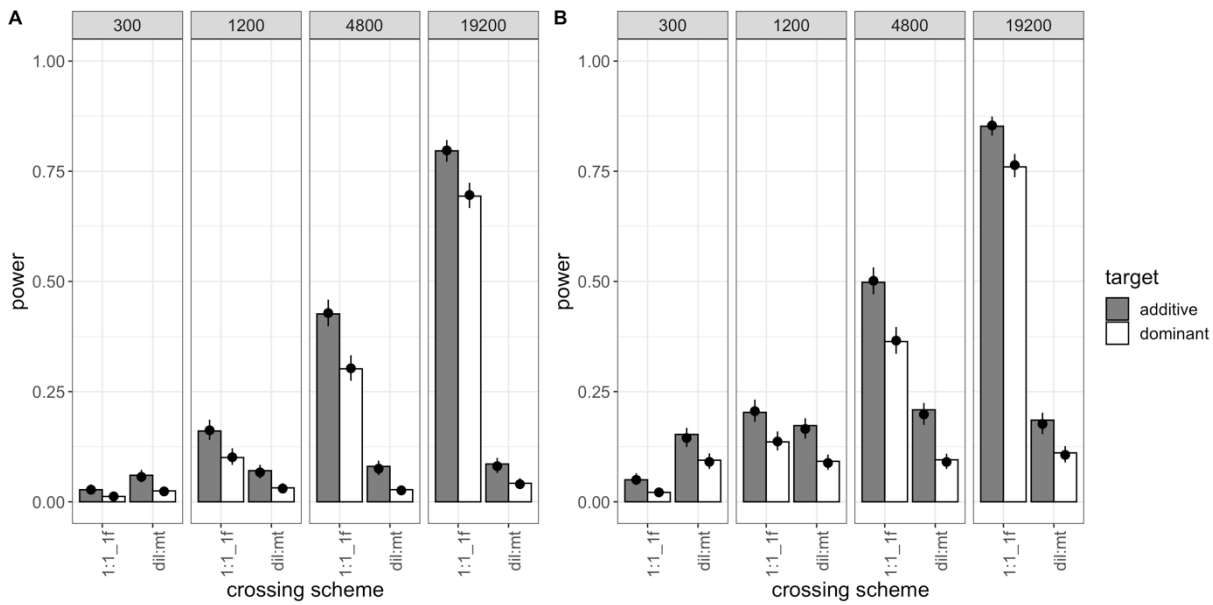

Figure S3. Power of the 1:1_1f and dil:mt crossing scheme at different population sizes (2,000 simulations/experimental design) after 20 generations of adaptation. Bars show the power (i.e., proportion of successful simulations) separately for each combination of crossing scheme (1:1_1f, dil:mt), population size (300; 1,200; 4,800; 19,200 individuals), and dominance coefficient (additive in grey, dominant in white). The dots with error bars display the model fit (Model 1) and its 95 % confidence interval. For the model fit, the selection coefficient was fixed to its global average, and combination-specific average starting allele frequencies were used. (A) shows the results for success-A (= selection target is the SNP with the highest Cochran-Mantel-Haenszel (CMH) test statistic) (B) shows the results for success-B (= selection target is not more than 100 SNPs away from the SNP with the highest CMH test statistic).

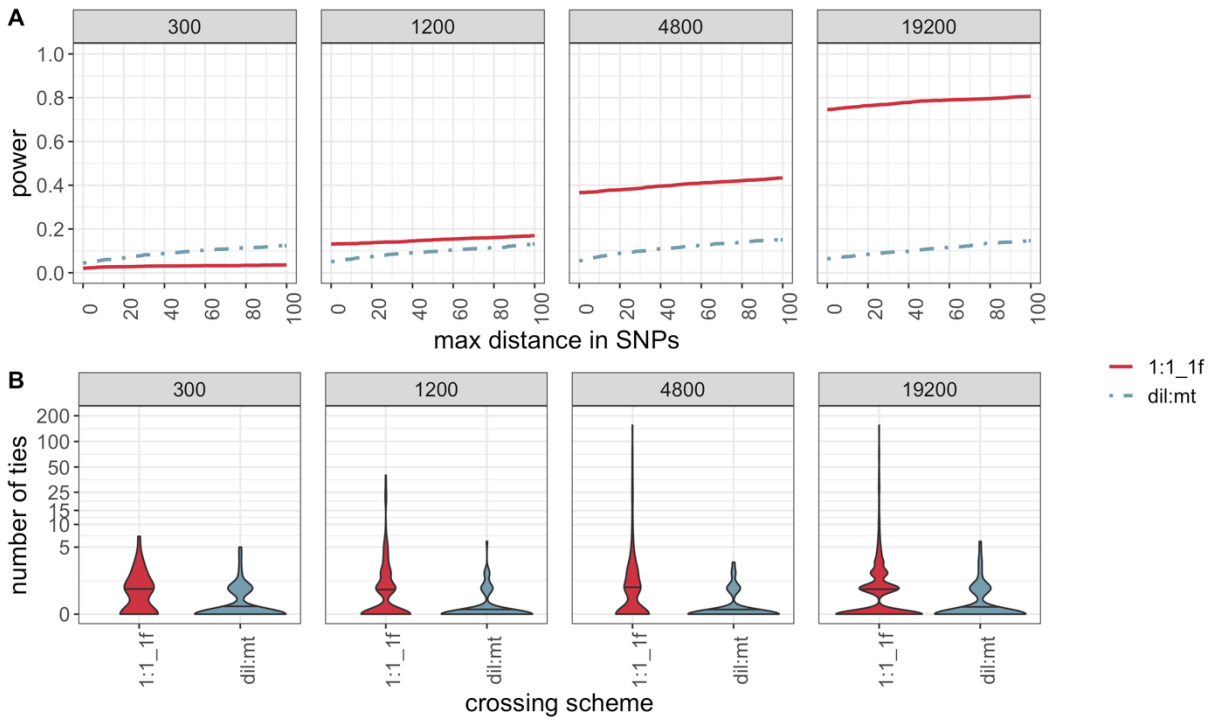

Figure S4. Resolution for the 1:1_1f and dil:mt crossing scheme simulated with different population sizes after 20 generations of adaptation. (A) Proportion of simulations (y-axis) that do not exceed a maximum distance in SNPs (x-axis) between the SNP with the highest Cochran-Mantel-Haenszel (CMH) test statistic and the true target of selection (B) Violin plots of the number of ties (y axis = log10 (number of ties + 1)) for simulations where the true target of selection has the highest CMH test statistic (success-A). The black horizontal lines in the violin plots display the median number of observed ties. Ties are defined as neighboring SNPs that have the same CMH test statistic as the target of selection.

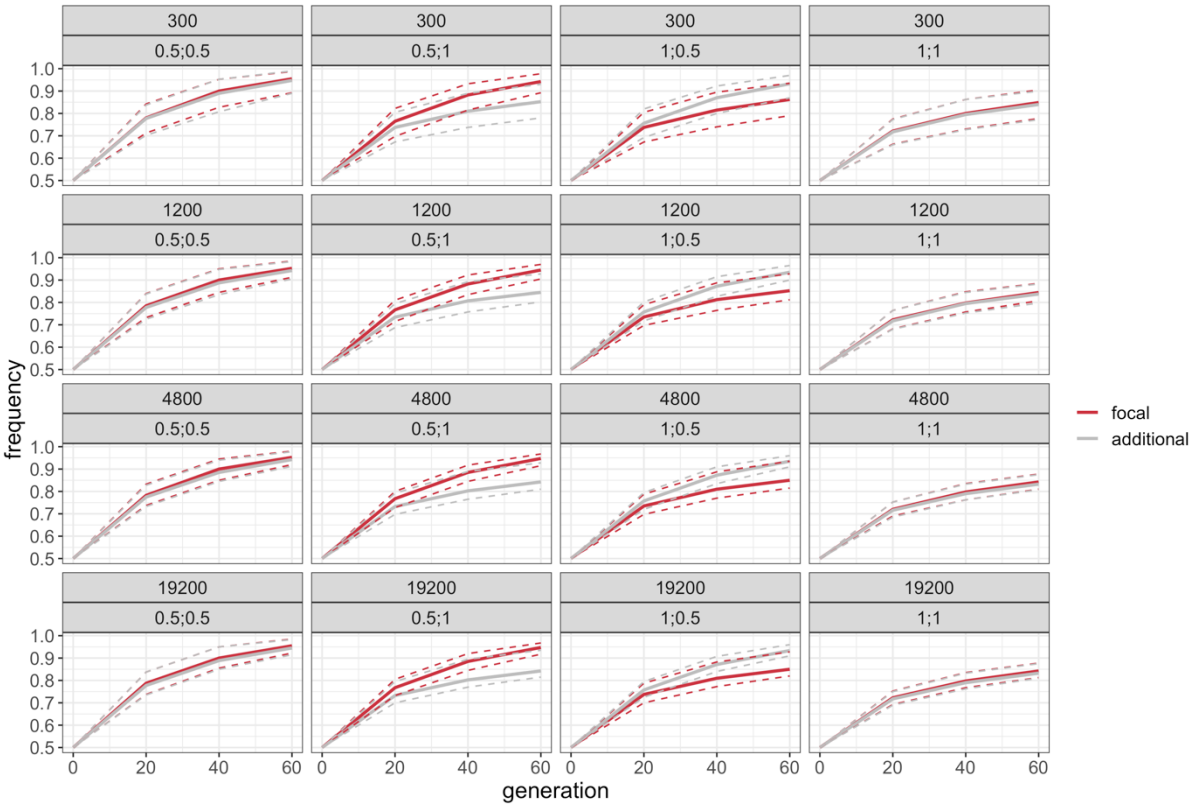

Figure S5. Median allele frequency trajectory of focal (red) and additional targets (grey) in 1:1_2f. For each single simulation, the target frequencies of a distinct generation were averaged over five replicates. Solid lines show the median allele frequency trajectory over 2,000 independent simulations per experimental design. Dashed lines show the 5 and 95 percentiles of the allele frequency trajectories. Each panel shows the median allele frequency trajectory of one particular dominance coefficient (focal target; additional target) and population size (300; 1,200; 4,800; 19,200 individuals) combination.

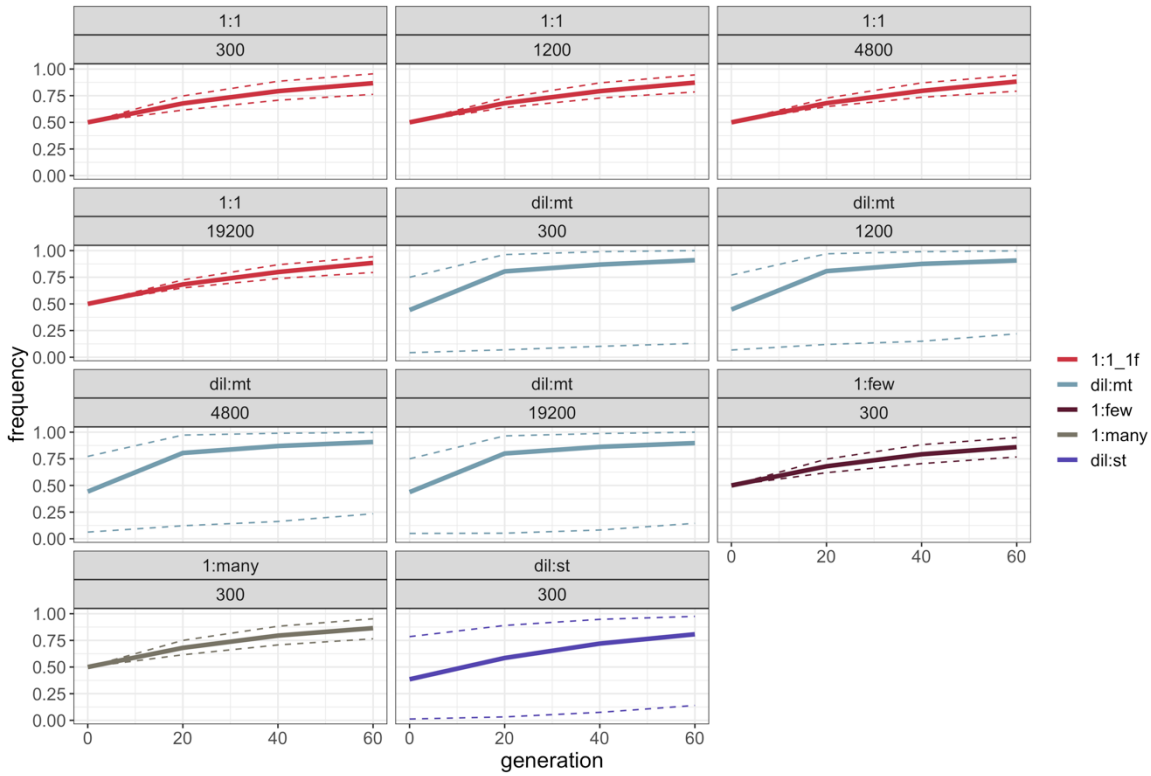

Figure S6. Median allele frequency trajectory of focal targets in different experimental designs. For each single simulation, the focal target frequency of a distinct generation was averaged over five replicates. Solid lines show the median allele frequency trajectory over 2,000 independent simulations per experimental design. Dashed lines show the 5 and 95 percentiles of the allele frequency trajectories. Each panel shows the median allele frequency trajectory of one particular crossing scheme (1:1_1f, dil:mt, 1:few, 1:many, dil:st) and population size (300; 1,200; 4,800; 19,200 individuals) combination.

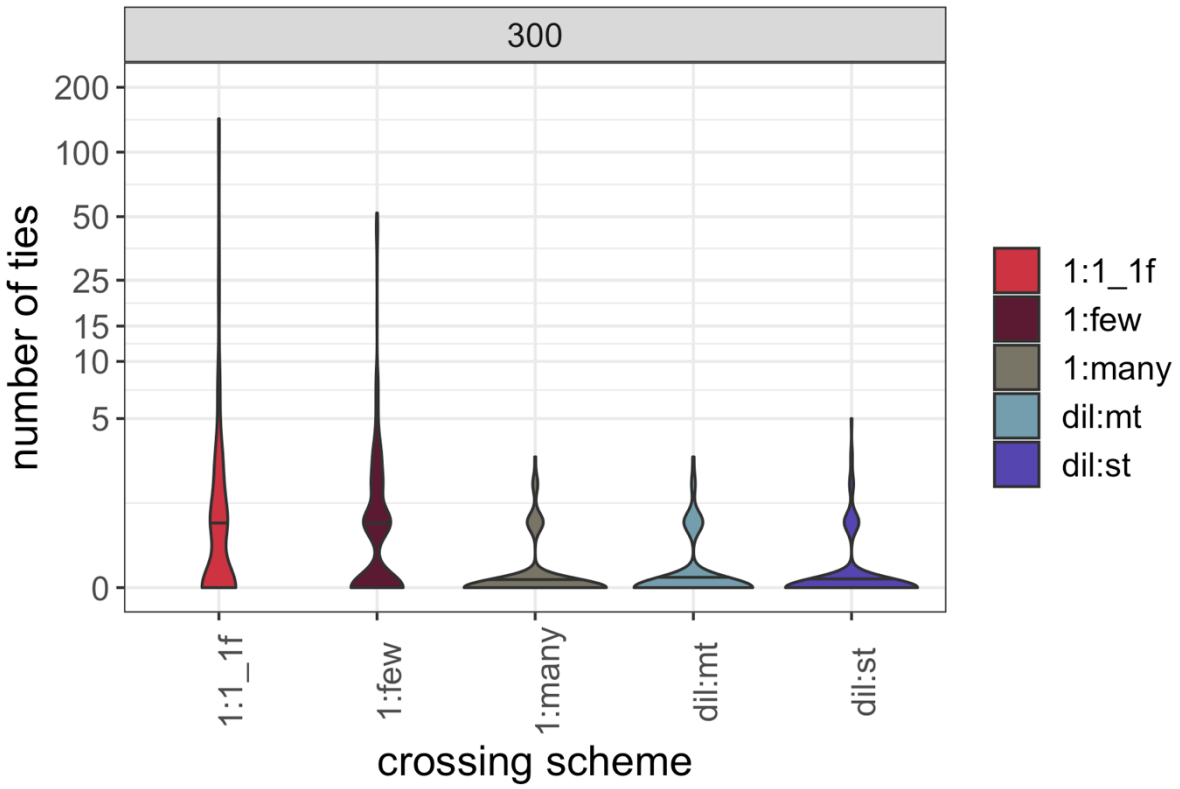

Figure S7. Violin plots of the number of ties (y axis = log10 (number of ties + 1)) for simulations where the true target of selection has the highest Cochran-Mantel-Haenszel (CMH) test statistic (success-A, population size = 300 individuals; 5 replicates; 2,000 simulations/experimental design). The black horizontal lines in the violin plots display the median number of observed ties. Ties are defined as neighboring SNPs that have the same CMH test statistic as the target of selection.

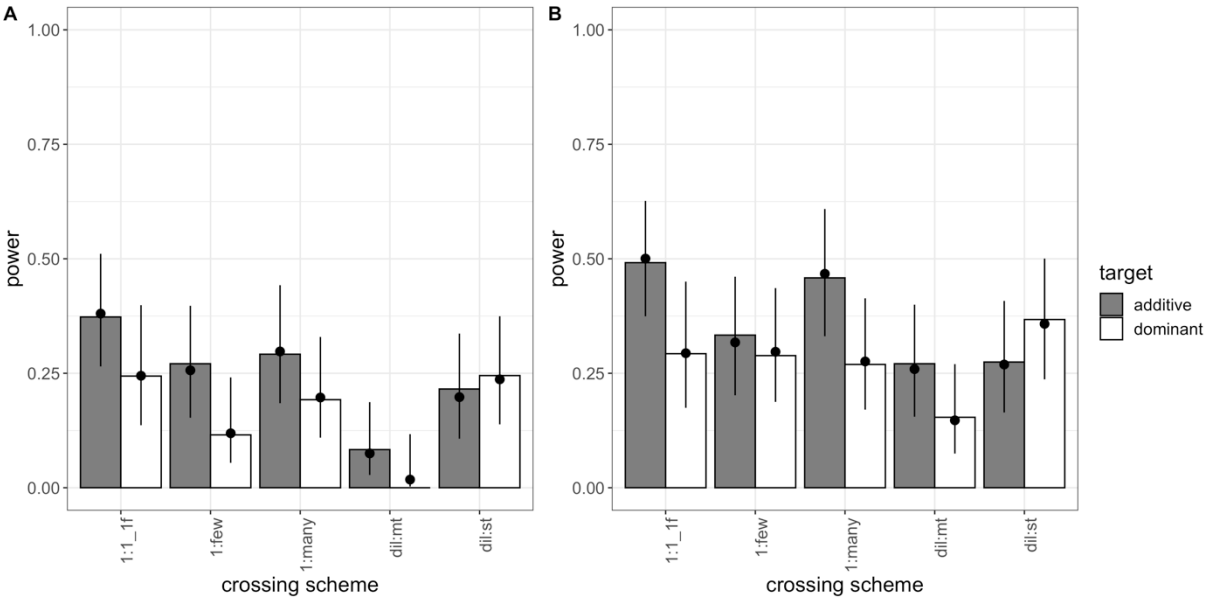

Figure S8. Power of five different crossing schemes (population size = 300 individuals; 30 replicates; 100 simulations/experimental design). Bars show the power (i.e., proportion of successful simulations) separately for each combination of crossing scheme and dominance coefficient (additive in grey; dominant in white). The dots with error bars display the estimate from the fitted model (Model 3) and its 95 % confidence interval. For the model fit, the selection coefficient was fixed to its global average, and combination-specific average starting allele frequencies were used. (A) shows the results for success-A (= selection target is the SNP with the highest Cochran-mantel-Haenszel (CMH) test statistic), (B) shows the results for success-B (= selection target is not more than 100 SNPs away from the SNP with the highest CMH test statistic).

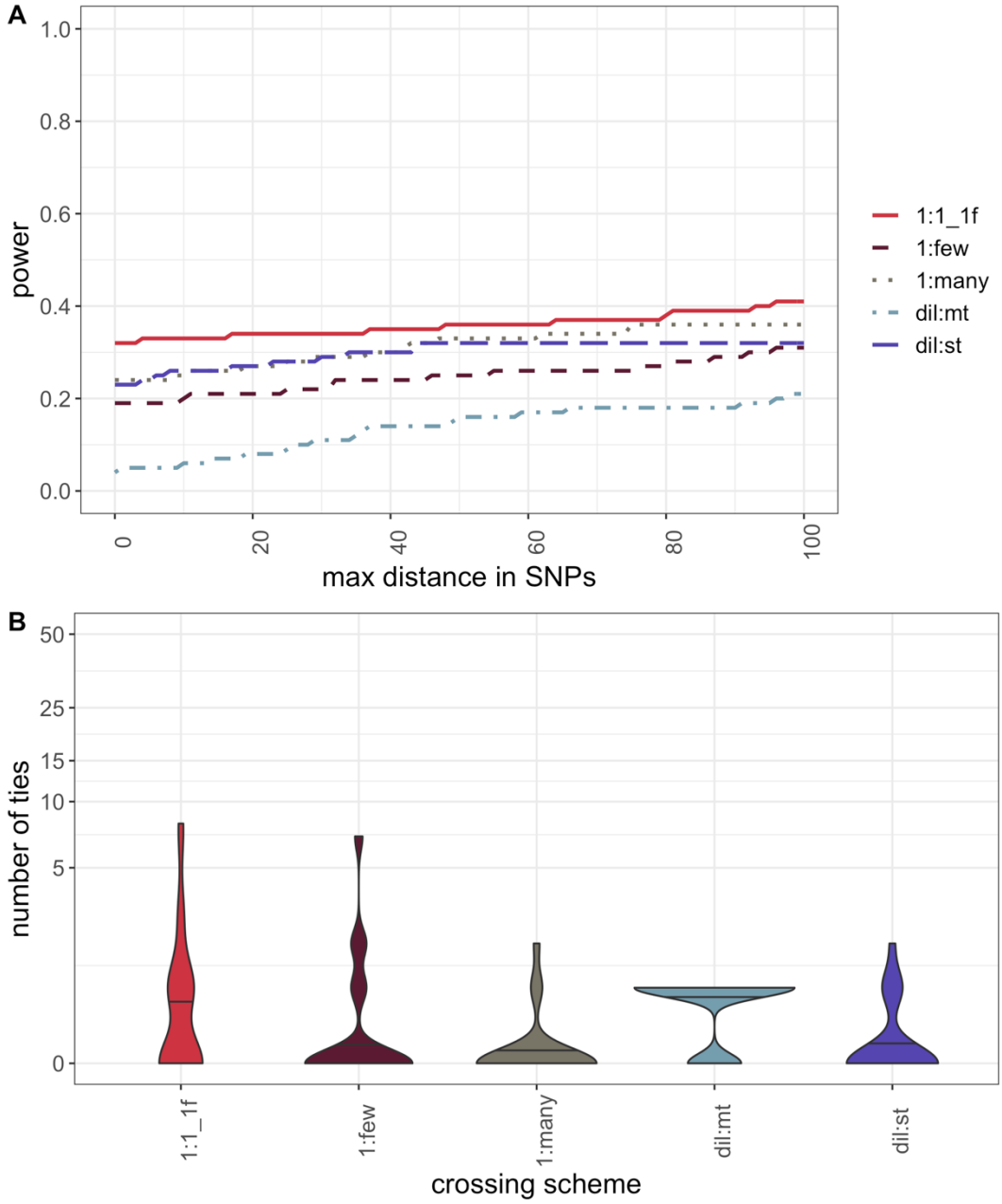

Figure S9. Resolution for five different crossing schemes (population size = 300 individuals; 30 replicates; 100 simulations/experimental design). (A) Proportion of simulations (y-axis) that do not exceed a maximum distance in SNPs (x-axis) between the SNP with the highest Cochran-Mantel-Haenszel (CMH) test statistic and the true target of selection (B) Violin plots of the number of ties (y axis = $\log_{10}$ (number of ties + 1)) for simulations where the true target of selection has the highest CMH test statistic (success-A). The black horizontal lines in the violin plots display the median number of observed ties. Ties are defined as neighboring SNPs that have the same CMH test statistic as the target of selection.

84 **Supplementary Tables**

85

86 **Table S1.** Number of SNPs per crossing scheme.

87 **Table S2.** Type II ANOVA (Model 1).

88 **Table S3.** Nagelkerke's R^2-index (Model 1).

89 **Table S4.** Type II ANOVA (Model 2).

90 **Table S5.** Nagelkerke's R^2-index (Model 2).

91 **Table S6.** Type II ANOVA (Model 3).

92 **Table S7.** Nagelkerke's R^2-index (Model 3).

93 **Table S1.** Number of SNPs per crossing scheme on chromosome-arm 2L.

crossing scheme	median	range
1:1	523,008	479,507 – 527,771
1:few	526,510	522,470 – 530,230
1:many	970,466	970,466 – 970,466
dil:mt	970,466	970,466 – 970,466
dil:st	970,466	970,466 – 970,466

94

Table S2. Type II ANOVA of explanatory variables for the analysis of success in secondary Evolve and Resequence studies with model 1 after 60 and 20 generations of adaptation. cross= crossing scheme; h= dominance coefficient; s= selection coefficient; af= mean starting allele frequency of the focal target over 5 replicates; N= population size; cross:h = interaction term between crossing scheme and dominance coefficient; h:af = interaction term between dominance coefficient and mean starting allele frequency; cross:N = interaction term between crossing scheme and population size ; h:N = interaction term between dominance coefficient and population size; cross:h:N = interaction term between crossing scheme, dominance coefficient, and population size.

generations	**term**	**df**	χ^2	***P***	χ^2	***P***
			success-A		**success-B**	
60	cross*	1	3188.7	<0.001	2514.70	<0.001
	h*	1	687.5	<0.001	652.41	<0.001
	s [1]	1	67.4	<0.001	73.39	<0.001
	af*[1]	1	3.9	0.048	0.69	0.407
	N*	3	1791.3	<0.001	1898.77	<0.001
	cross:h	1	2.1	0.145	8.24	0.004
	h:af	1	18.5	<0.001	16.67	<0.001
	cross:N	3	315.5	<0.001	677.98	<0.001
	h:N	3	6.8	0.079	2.70	0.440
	cross:h:N	3	3.8	0.286	16.12	0.001
20	cross*	1	2079.94	<0.001	1056.48	<0.001
	h*	1	139.04	<0.001	181.36	<0.001
	s [1]	1	18.21	<0.001	58.96	<0.001
	af* [1]	1	39.91	<0.001	77.13	<0.001
	N*	3	2589.34	<0.001	2204.36	<0.001
	cross:h	1	3.73	0.053	1.15	0.284
	h:af	1	0.02	0.898	0.36	0.551
	cross:N	3	573.81	<0.001	1156.81	<0.001
	h:N	3	0.58	0.900	0.87	0.833
	cross:h:N	3	1.29	0.732	4.68	0.197

* In type II ANOVA, main effects are not corrected for the interaction part of the model, while interaction terms are corrected for the main effects in the model.

[1] multiplied by 100, and z-transformed to mean = 0, and sd =1; Mean/standard deviation of the original value was 0.463/0.130 for the starting allele frequency, and 0.086/0.009 for the selection coefficient respectively

Table S3. Nagelkerke's R^2-index of each explanatory variable including all its interactions in the logistic regression (Model 1). If the reduced model explains the data as well as a full model that includes the evaluated effect, Nagelkerke's R^2-index is 0.

generations	**effect**	**R^2 success-A**	**R^2 success-B**
60	crossing scheme	0.305	0.264
	dominance coefficient	0.077	0.069
	selection coefficient	0.007	0.007
	mean starting allele frequency	0.003	0.002
	population size	0.204	0.224
20	crossing scheme	0.283	0.211
	dominance coefficient	0.019	0.021
	selection coefficient	0.002	0.007
	mean starting allele frequency	0.005	0.009
	population size	0.322	0.295

Table S4. Type II ANOVA of explanatory variables for the analysis of success in secondary Evolve and Resequence studies with model 2. architecture= version of the 1:1 crossing scheme in combination with the dominance coefficient of the additional target; h= dominance coefficient of the selection target of interest; s= selection coefficient; N= population size; architecture:h = interaction term between architecture and dominance coefficient of the selection target of interest; architecture:N = interaction term between architecture and population size ; h:N = interaction term between dominance coefficient of the selection target of interest and population size; architecture:h:N = interaction term between architecture, dominance coefficient of the selection target of interest, and population size.

term	**df**	χ^2	***P***	χ^2	***P***
		success-A		**success-B**	
architecture*	4	855.4	<0.001	1509.9	<0.001
h*	1	2742.4	<0.001	2755.9	<0.001
s [1]	1	181.9	<0.001	137.5	<0.001
N*	3	5230.6	<0.001	6661.9	<0.001
architecture:h	4	697.8	<0.001	708.6	<0.001
architecture:N	12	17.5	0.132	42.7	<0.001
h:N	3	12.3	0.006	3.0	0.399
architecture:h:N	12	27.9	0.006	29.8	0.003

* In type II ANOVA, main effects are not corrected for the interaction part of the model, while interaction terms are corrected for the main effects in the model.

[1] multiplied by 100, and z-transformed to mean = 0, and sd =1; Mean/standard deviation of the original value was 0.085/0.009.

Table S5. Nagelkerke's R^2-index of each explanatory variable including all its interactions in the logistic regression (Model 2). If the reduced model explains the data as well as a full model that includes the evaluated effect, Nagelkerke's R^2-index is 0.

effect	**R^2 success-A**	**R^2 success-B**
architecture	0.107	0.158
dominance coefficient	0.201	0.210
selection coefficient	0.012	0.009
population size	0.285	0.348

126 **Table S6.** Type II ANOVA of explanatory variables for the analysis of success in secondary Evolve and
127 Resequence studies with model 3. cross= crossing scheme; h= dominance coefficient; s= selection coefficient; af=
128 mean starting allele frequency of the focal target over 5 replicates; cross:h= interaction term between crossing
129 scheme and dominance coefficient; h:af= interaction term between dominance coefficient and mean starting allele
130 frequency.

generations	**term**	**df**	χ^2	***P***	χ^2	***P***
			success-A		**success-B**	
5	cross*	4	218.65	<0.001	93.01	<0.001
	h*	1	371.35	<0.001	321.13	<0.001
	s [1]	1	76.20	<0.001	72.09	<0.001
	af* [1]	1	5.55	0.019	12.66	<0.001
	cross:h	4	77.19	<0.001	97.21	<0.001
	h:af	1	7.56	0.006	7.07	0.008
30	cross*	4	28.79	<0.001	11.28	0.024
	h*	1	5.13	0.024	4.40	0.036
	s [1]	1	2.63	0.105	3.65	0.056
	af* [1]	1	1.34	0.247	0.13	0.716
	cross:h	4	2.68	0.612	5.41	0.247
	h:af	1	1.73	0.189	1.01	0.315

131 * In type II ANOVA, main effects are not corrected for the interaction part of the model, while interaction terms
132 are corrected for the main effects in the model.
133 [1] multiplied by 100, and z-transformed to mean = 0, and sd =1; Mean/standard deviation of the original value
134 were 0.463/0.133 for the starting allele frequency, and 0.085/0.009 for the selection coefficient respectively.

135 **Table S7.** Nagelkerke's R^2-index of each explanatory variable including all its interactions in the logistic
136 regression (Model 3). If the reduced model explains the data equally well as a full model that includes the evaluated
137 effect, Nagelkerke's R^2-index is 0.

replicates	**effect**	**R^2 success-A**	**R^2 success-B**
5	crossing scheme	0.061	0.033
	dominance	0.095	0.076
	selection coefficient	0.016	0.013
	starting allele frequency	0.003	0.004
30	crossing scheme	0.097	0.046
	dominance	0.034	0.034
	selection coefficient	0.009	0.010
	starting allele frequency	0.010	0.003

138